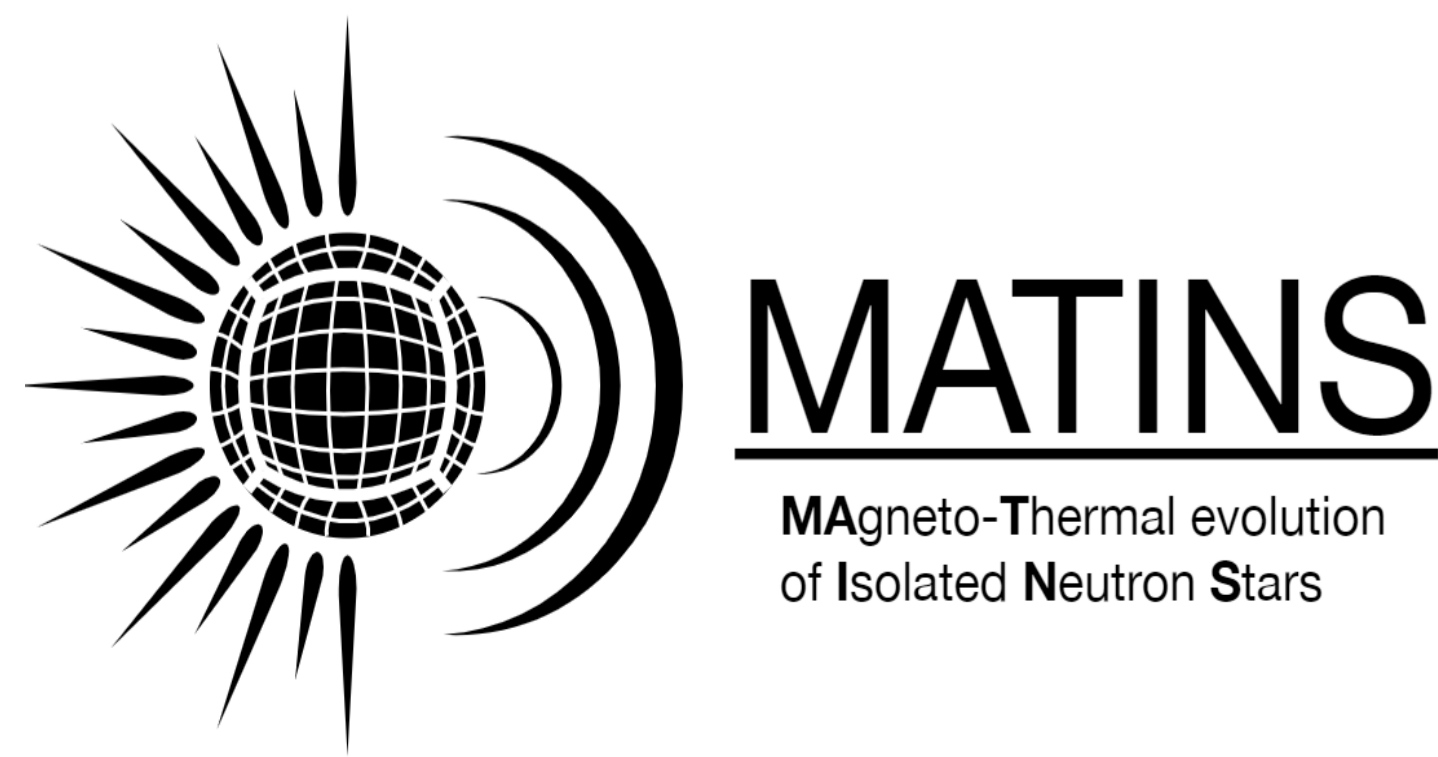


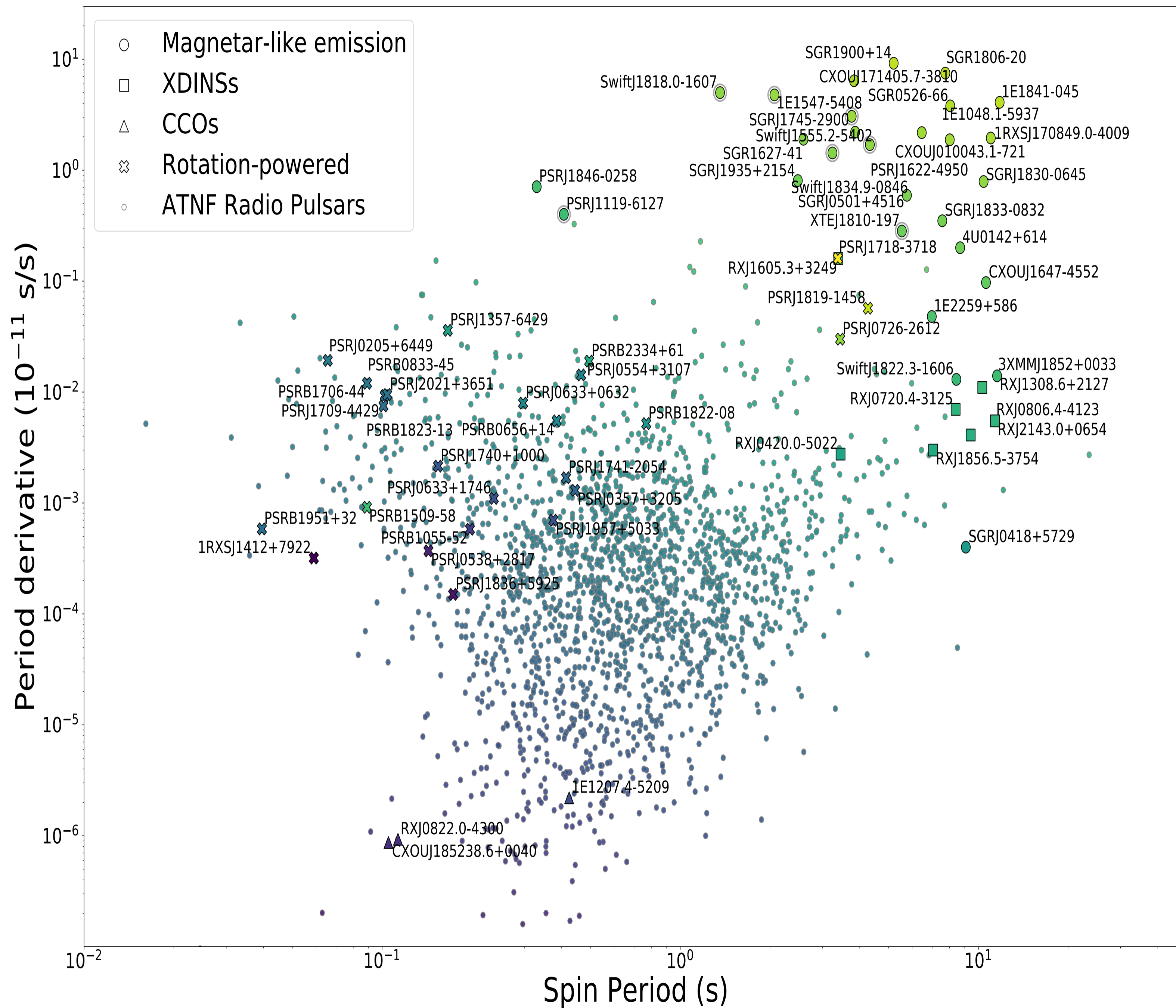
The physics governing magnetic field evolution in magnetars



June 4, 2026
ICE-CSIC, Barcelona
NewAthena Rising: SWG4

Clara Dehman
clara.dehman@ua.es
Juan de la Cierva Fellow

P-Pdot diagram for isolated neutron stars



Neutron stars form are observed across the electromagnetic spectrum

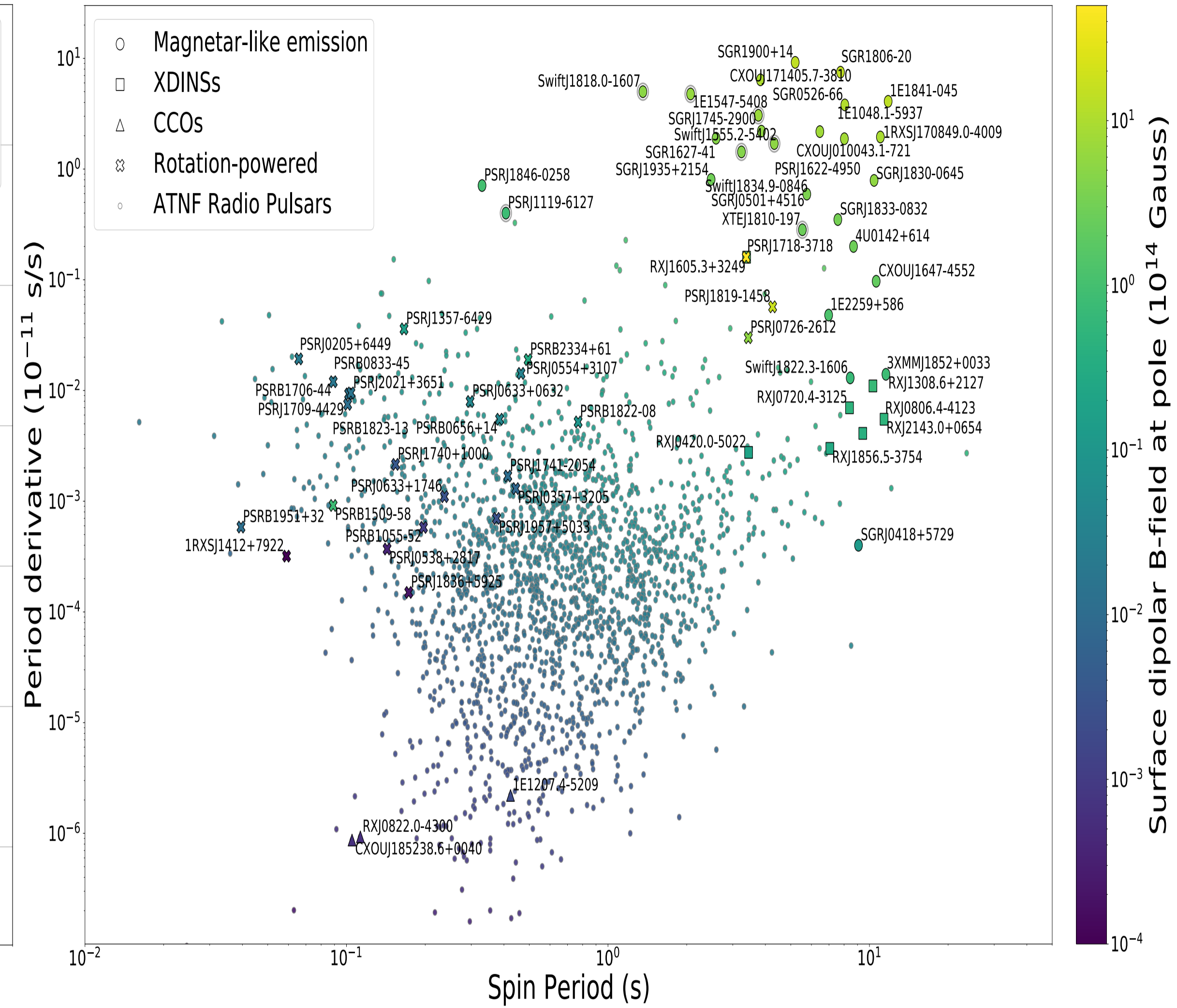
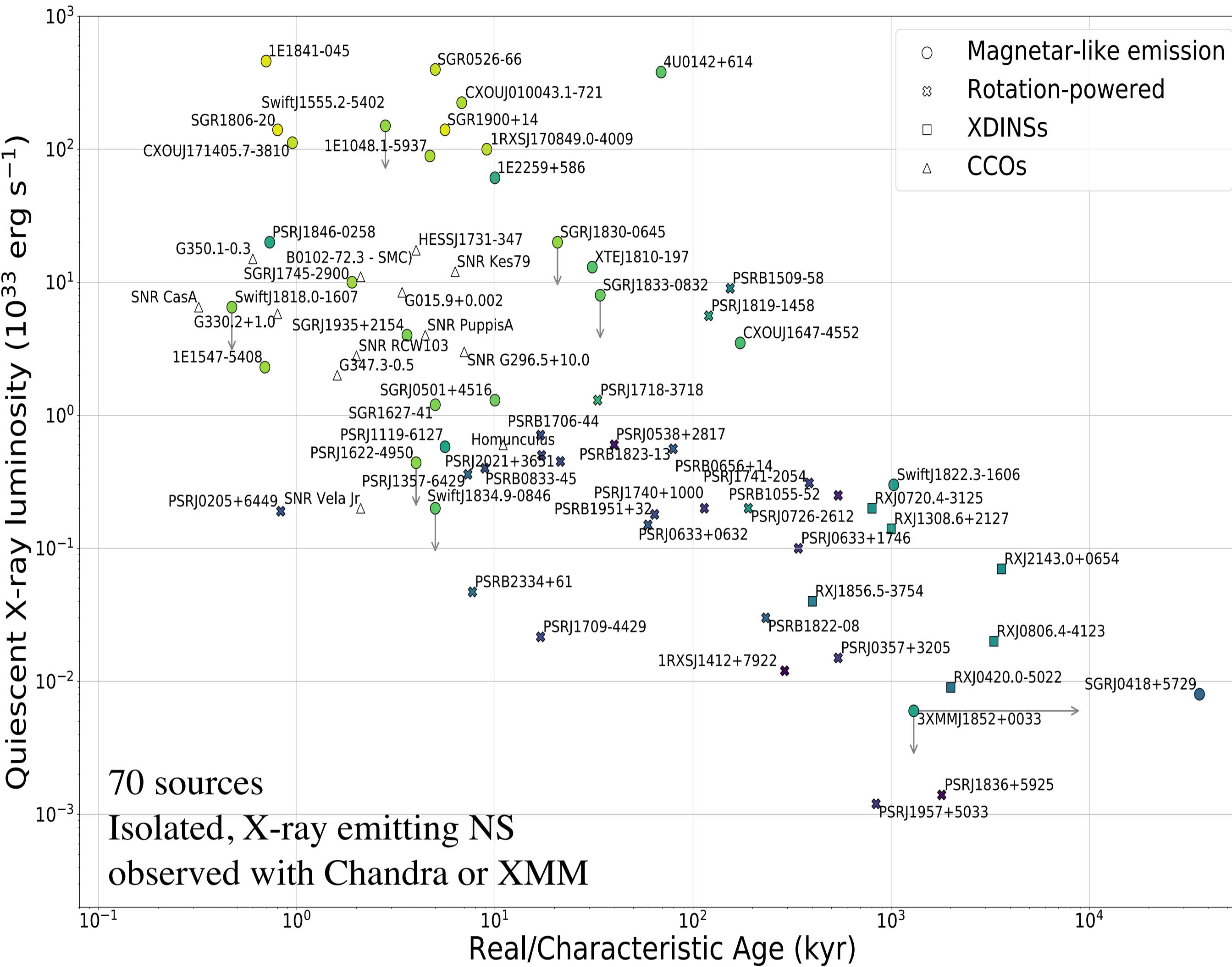
Dipolar magnetic field at the pole of the star:

$$B_{dip} = 6.4 \times 10^{19} \sqrt{P\dot{P}}$$

Characteristic age:

$$\tau_c = \frac{P}{2\dot{P}}$$

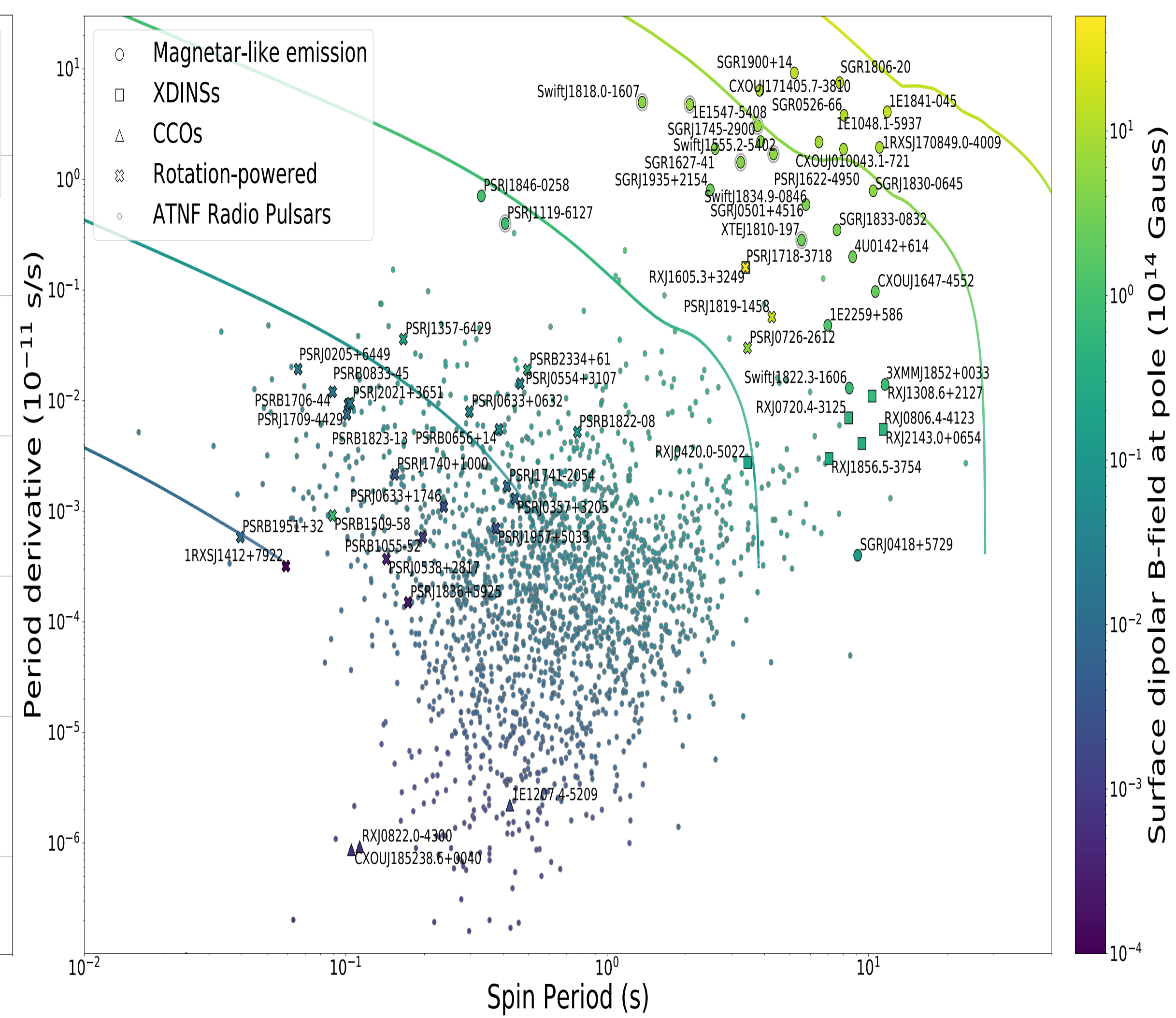
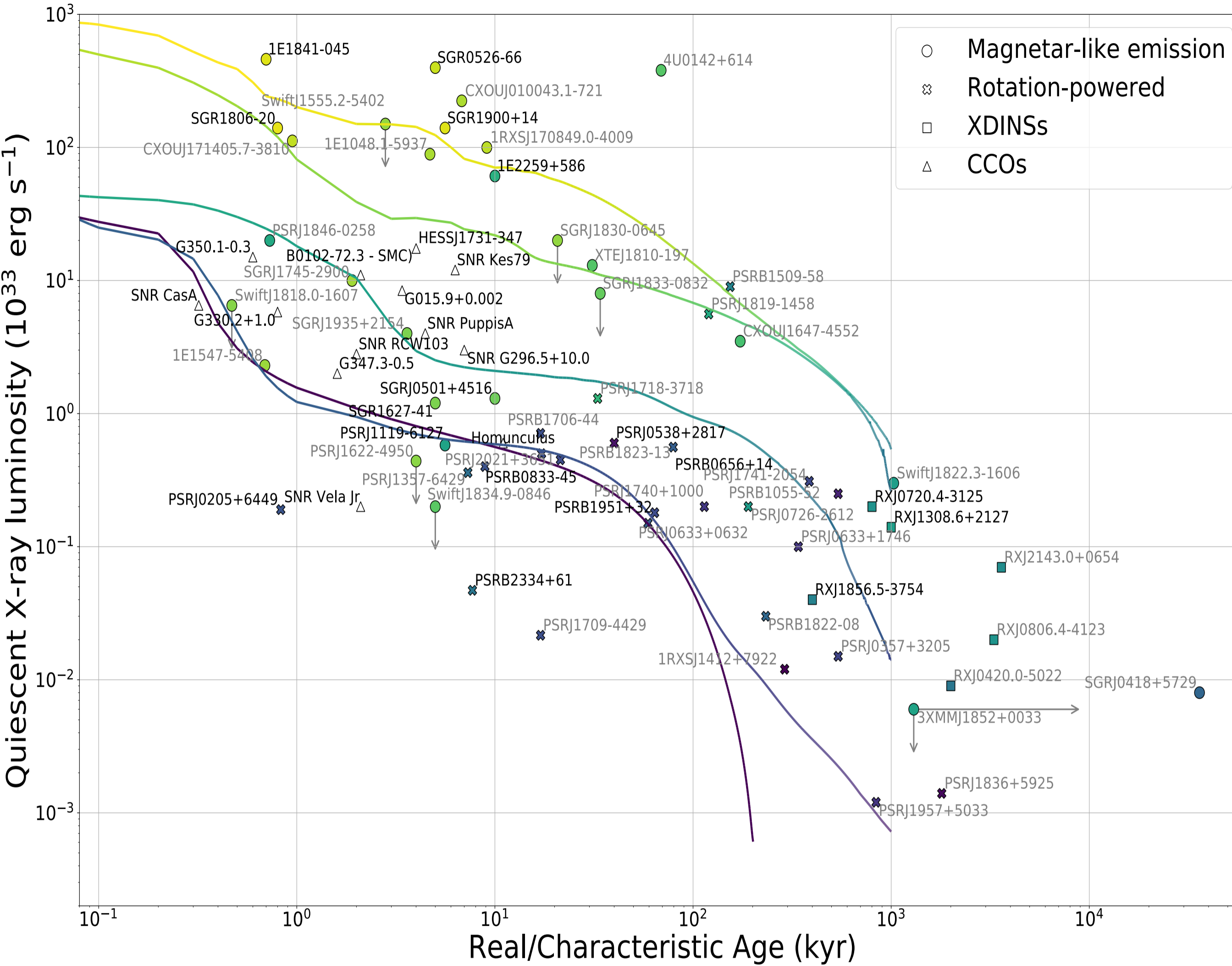
Observations: thermal X-ray luminosity, real age, P and Pdot



Four independent measured parameters.

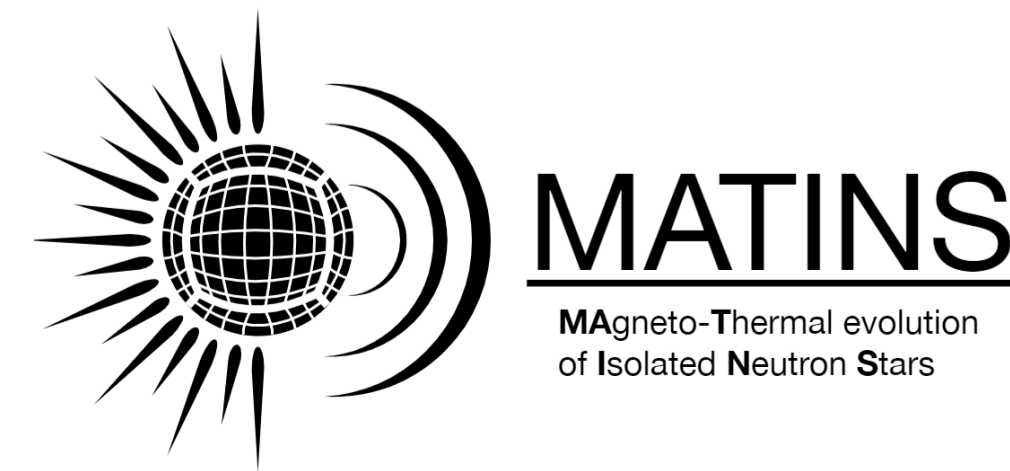
“Need for coupled magneto-thermal simulations to explain the luminosity and the evolution path of different isolated neutron stars” — [Viganò et al. 2013].

Why we need 3D magneto-thermal models?



- Realistic magnetic topology: complex and non-axisymmetric
- The need to model cooling curves, that depend on the 3d configuration

*“New 3D code
 MATINS”*



MATINS the brand new 3D code

– Open Access: <https://github.com/ice-csic-astroexotic/MATINS>–

$$\frac{\partial \mathbf{B}}{\partial t} = -\nabla \times \left[\eta \nabla \times (e^\nu \mathbf{B}) - \eta k_5 \mathbf{B} + f_h \nabla \times (e^\nu \mathbf{B}) \times \mathbf{B} \right] c_V(T) \frac{\partial (Te^\nu)}{\partial t} = \vec{\nabla} \cdot (e^\nu \hat{\mathbf{k}} \cdot \vec{\nabla} (e^\nu T)) + e^{2\nu} (Q_J - Q_\nu)$$

Dehman, Viganò, Pons & Rea 2023, MNRAS (DOI: [10.1093/mnras/stac2761](https://doi.org/10.1093/mnras/stac2761)): Cubed-sphere grid + Magnetic formalism

Dehman, Viganò, Ascenzi, Pons & Rea 2023, MNRAS (DOI: [10.1093/mnras/stad1773](https://doi.org/10.1093/mnras/stad1773)): First 3D magneto-thermal simulation

Ascenzi, Viganò, Dehman, Pons & Rea, Perna 2024, MNRAS (DOI: [10.1093/mnras/stae1749](https://doi.org/10.1093/mnras/stae1749)): Thermal formalism

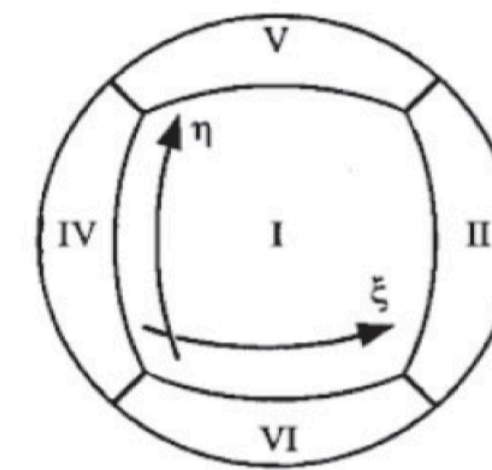
Dehman & Pons 2025, PRR (DOI: [10.1103/rhv5-nd4v](https://doi.org/10.1103/rhv5-nd4v)): Chiral magnetic effect

What's better than 2D (Viganò et al. 2021):

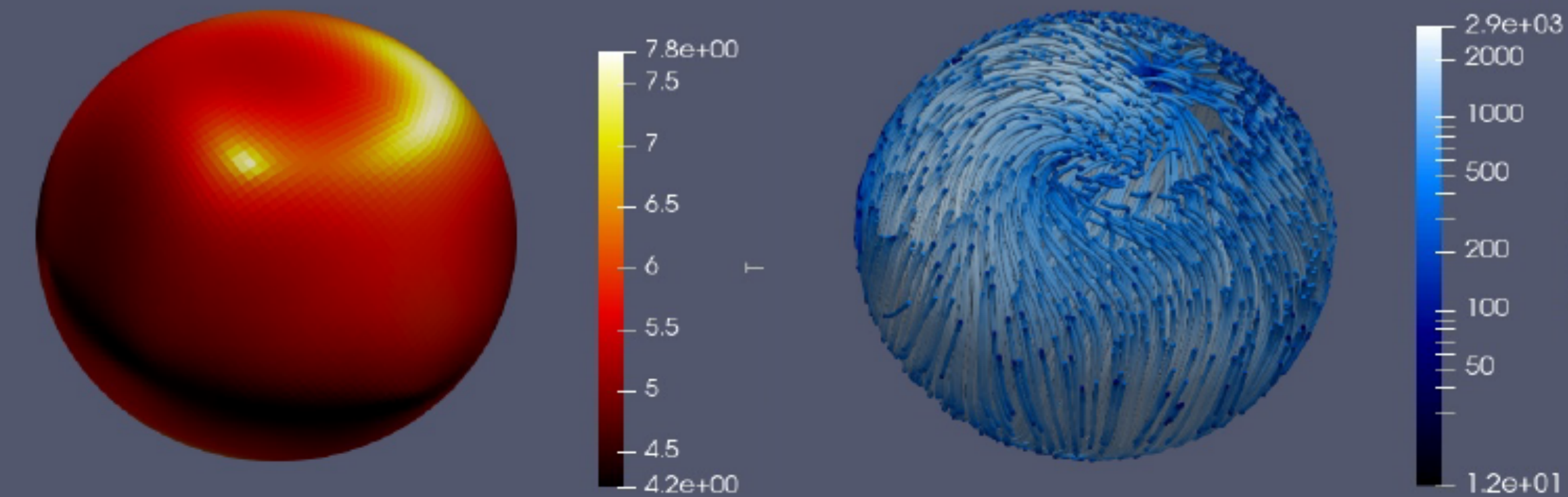
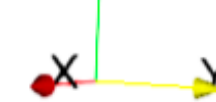
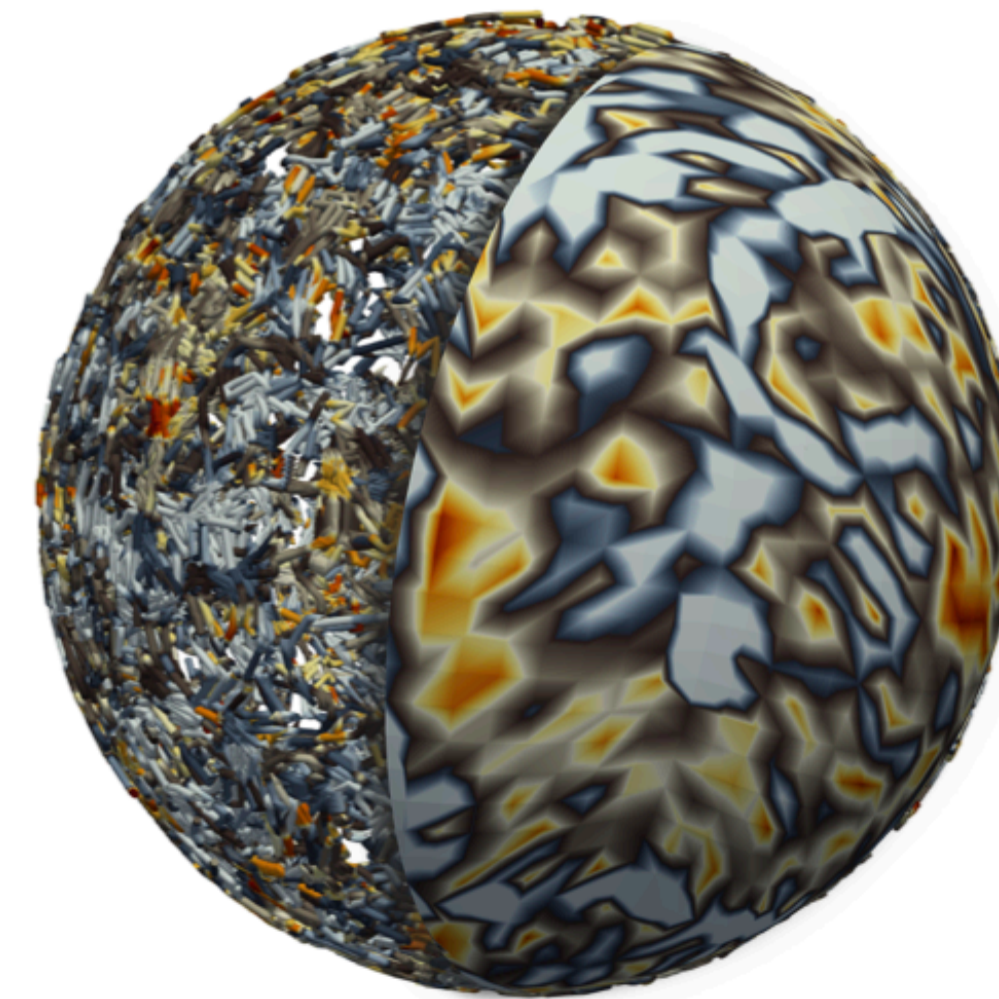
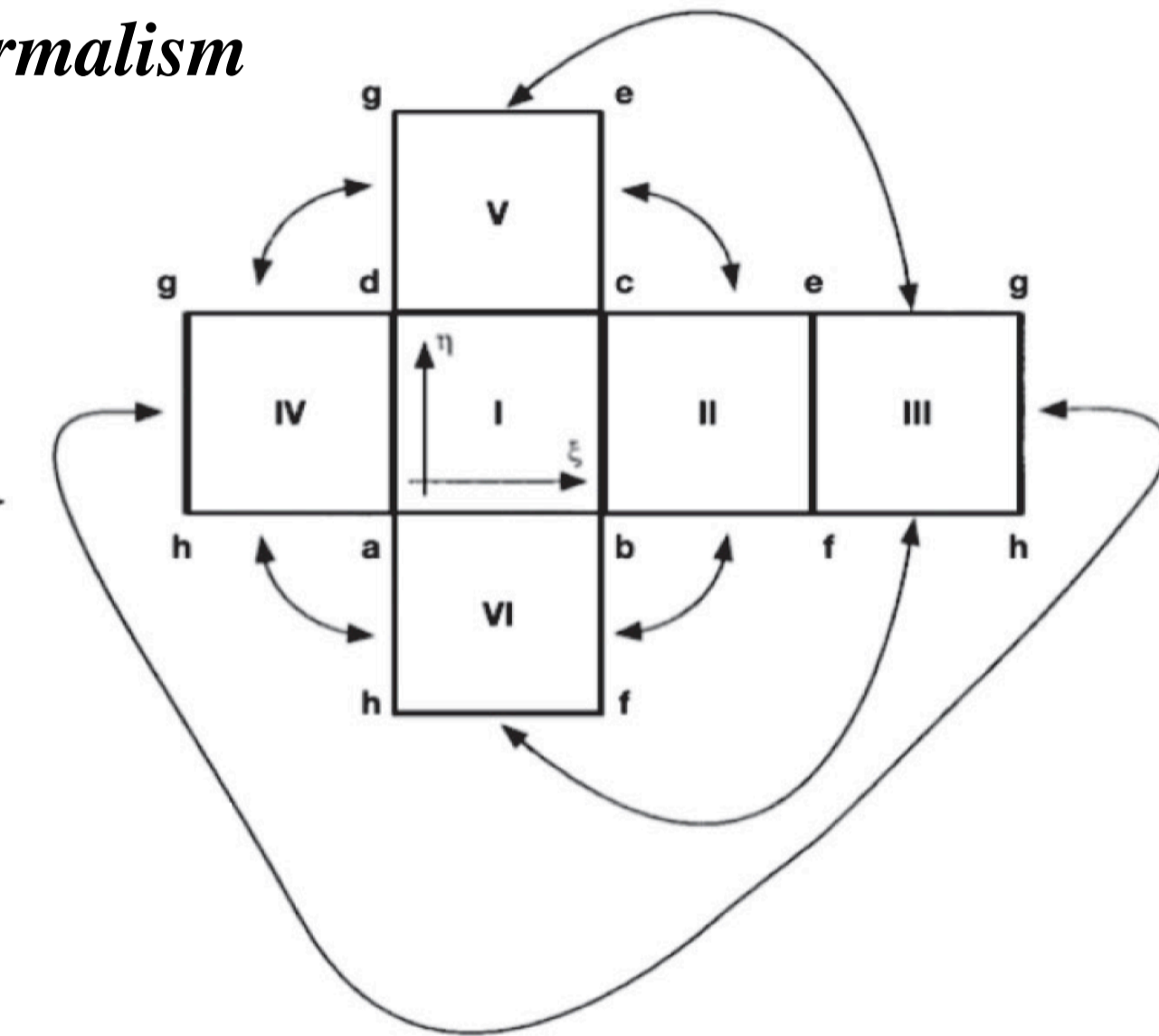
- Simulation of 3D magnetic modes, hotspots, and light curves
- Better documentation, **use of novel coordinates (cubed-sphere)**
- Optimization and use of OpenMP

Advance obtained:

- **Realistic 3D evolution and topology, appearance of hotspots**
- **State-of-the-art microphysics, various masses and EOSs, with realistic structure obtained by solving the TOV equation.**
- **Numerical scheme to better capture non-linear dynamics**
- **General relativistic correction**
- **State of art envelope model**
- **Flexibility in implementing new physics**

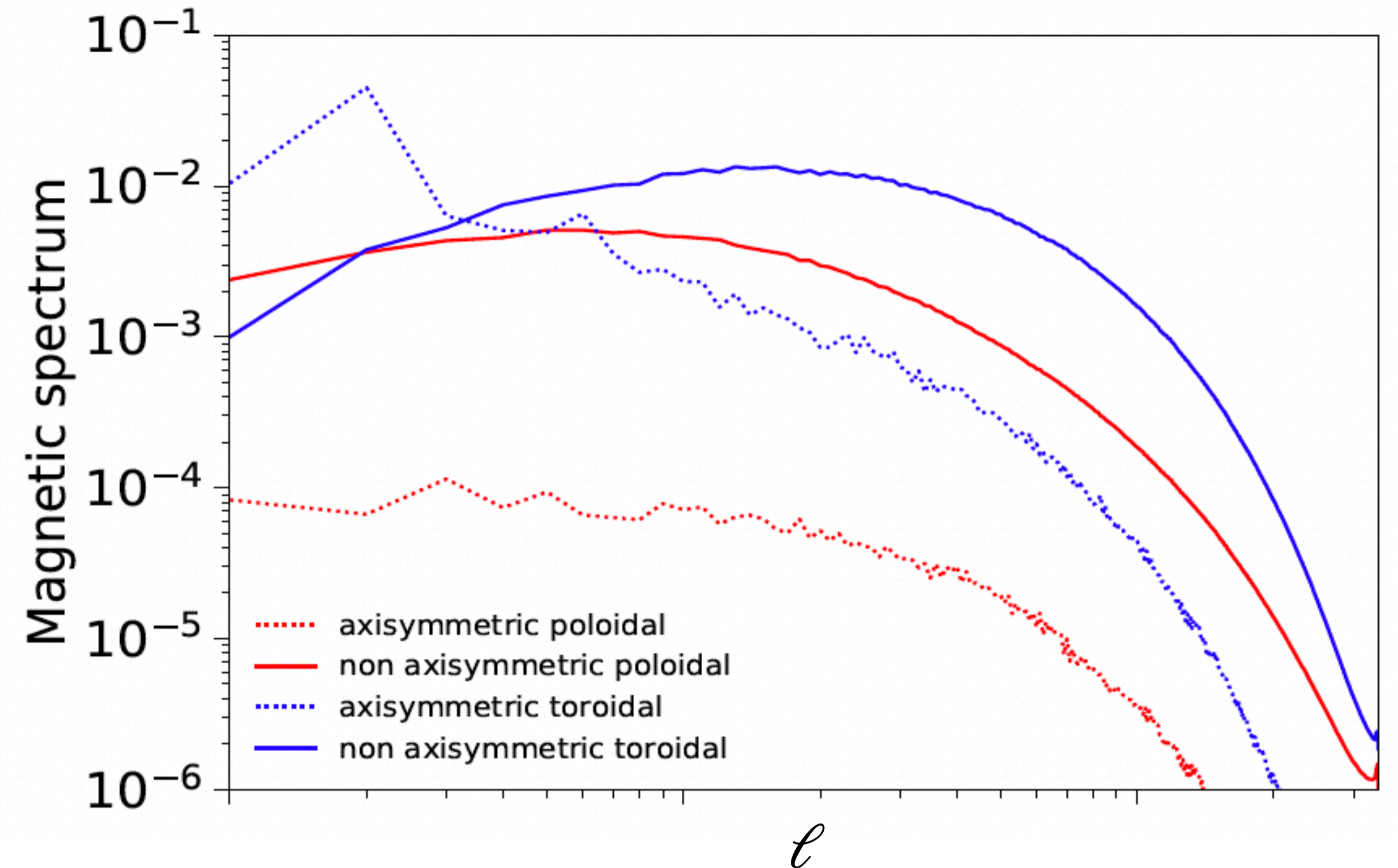
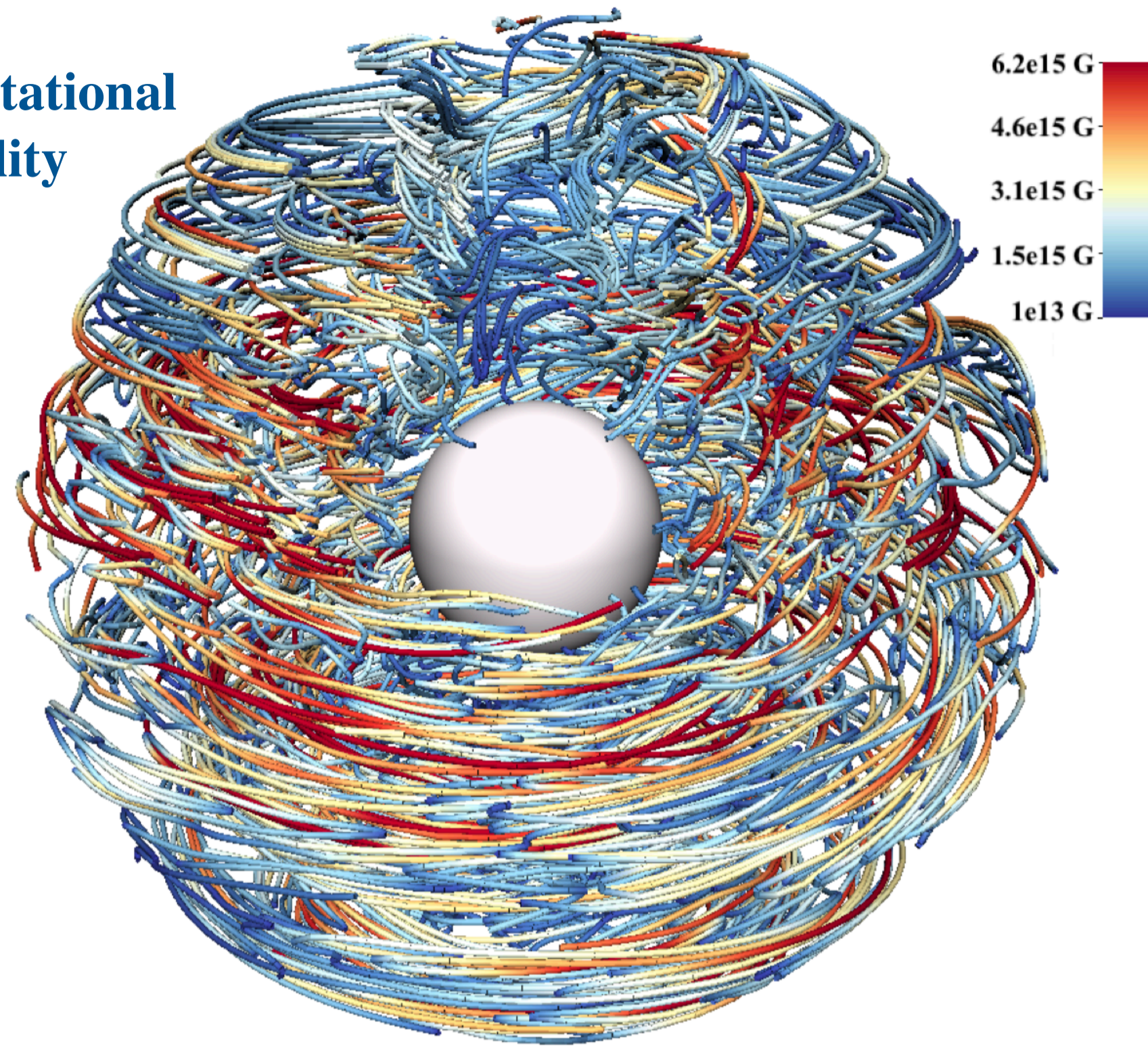


**cubed
sphere**



Magnetic field at birth: Magnetic spectrum after core-collapse

Magneto-rotational instability



Magnetic energy is distributed across a broad range of scales.

Toroidal axisymmetric quadrupole and non-axisymmetric components dominate.

Dipolar field accounts for less than 5% of the total magnetic energy ($\approx 10^{12}$ G).

From post-collapse to neutron star phase, plenty of MHD timescales to approach an equilibrium, with dynamo still going on and at the same time dissipating the smallest scales.

But how does a strong dipole of 10^{14} G form in magnetars, leading to their long spin periods?

[Reboul-Salze et al. 2022]

[Dehman et al. 2023c]

[Barrère et al. 2025]

[Igoshev et al. 2025]

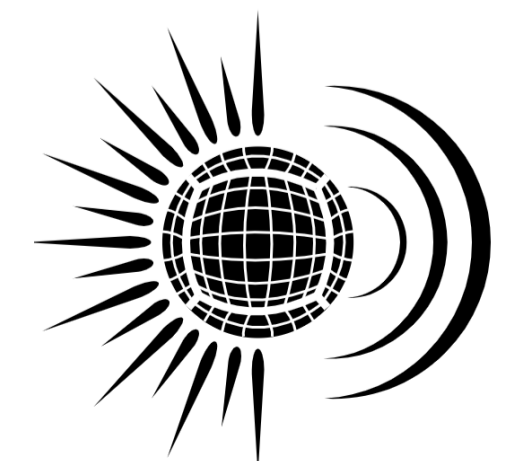
Magneto-rotational instability

Taylor-Spruit dynamo

Candidates to explain CCOs, low field magnetars



Weak dipolar component (order of 10^{12} G)



MATINS
MAgneto-Thermal evolution of Isolated Neutron Stars

Hall-driven inverse cascade in neutron star crusts

Initial field:

Helical magnetic field.

Random initial field peaking at $\ell_0 \sim 100$.

Causal spectrum as used in the cosmological context.

Correct aspect ratio of the NS crust.

Inverse Cascade occurs!

Energy transferred from small to large-scale multipoles.

Not observed in previous neutron star simulation studies.

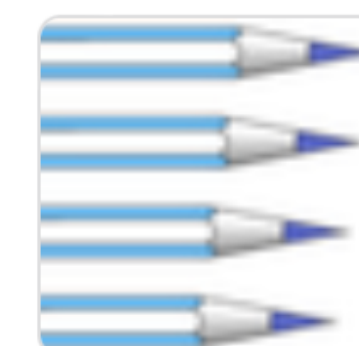
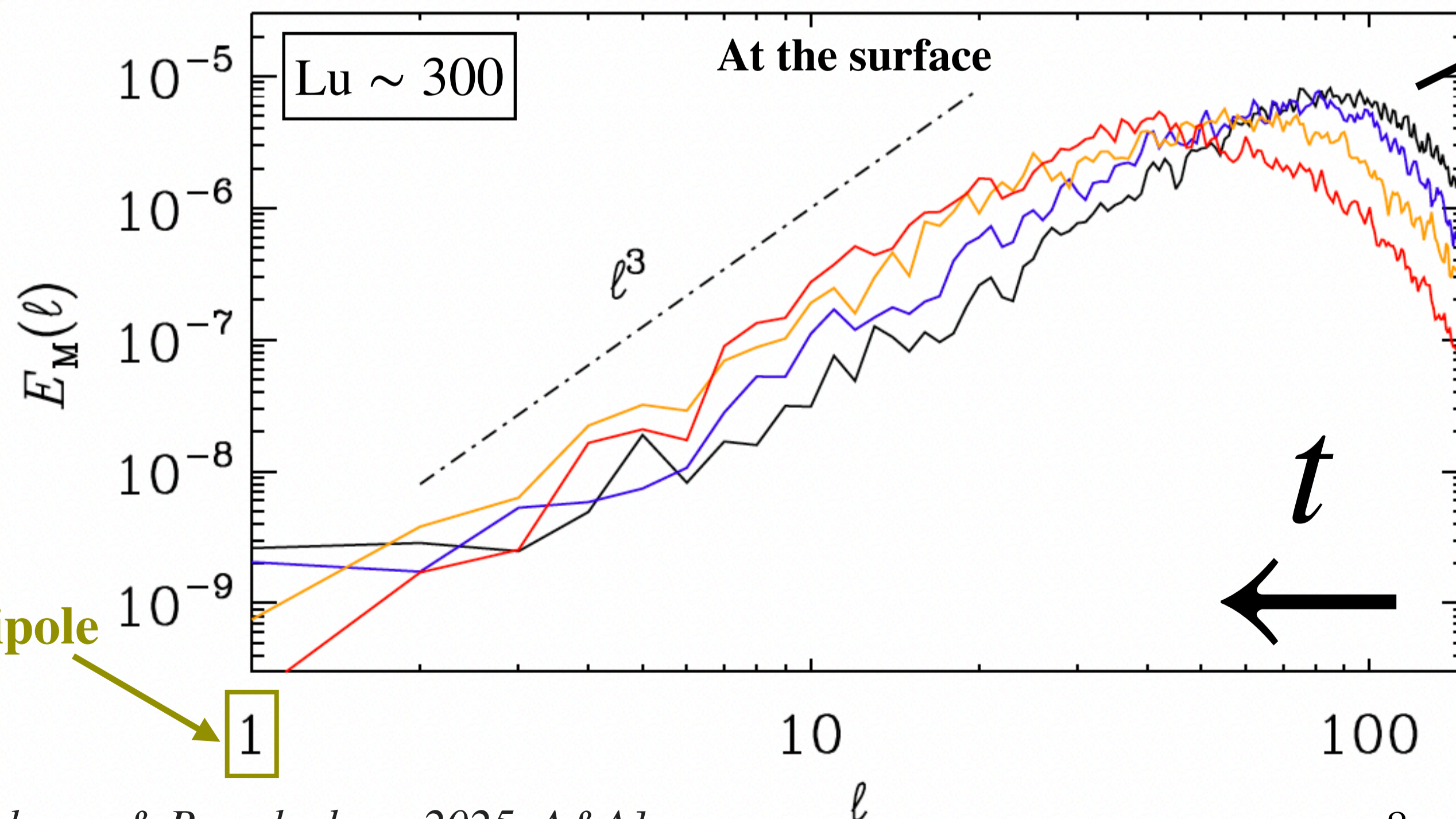
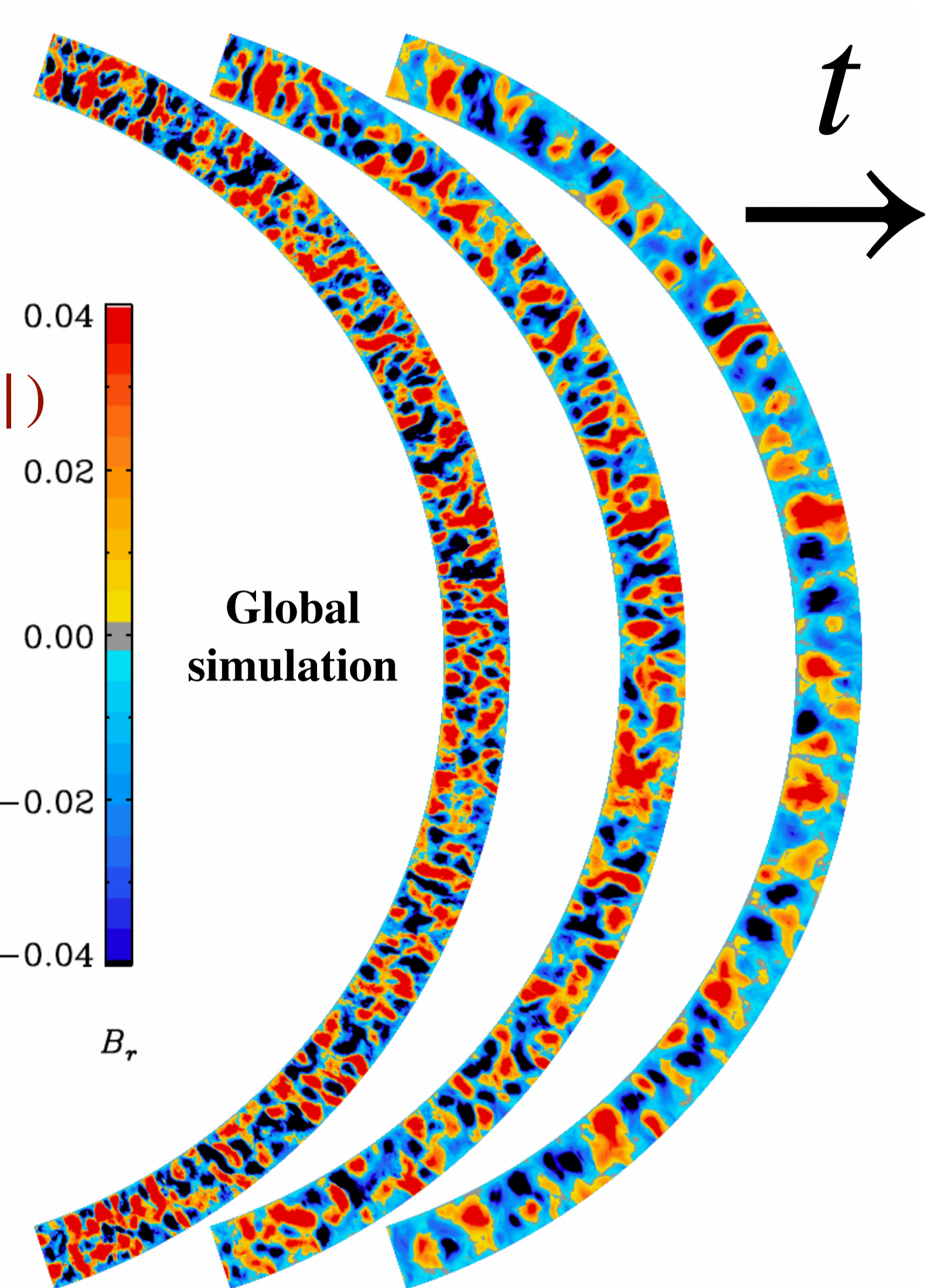
Extreme aspect ratio (1:30)—thin crust—limits the inverse cascade.

Maximally helical
(e.g., positive helicity):

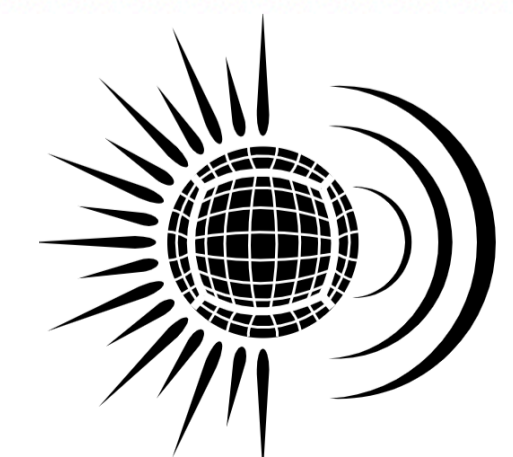
$$k = p + q$$

$$\begin{aligned} k |H_M(k)| / 2E_M(k) &\leq 1 \\ H_M &= 2E_M(k)/k \end{aligned}$$

$$|k| \leq \max(|p|, |q|)$$



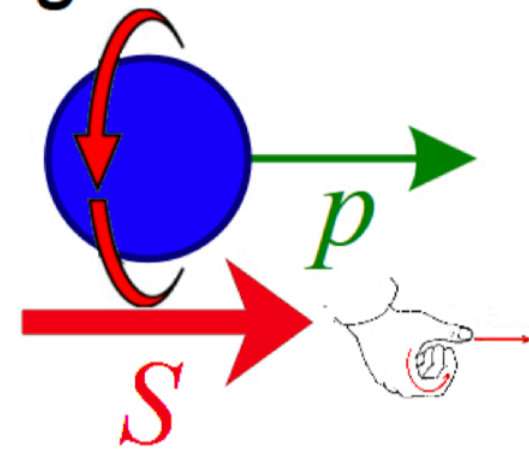
Pencil Code



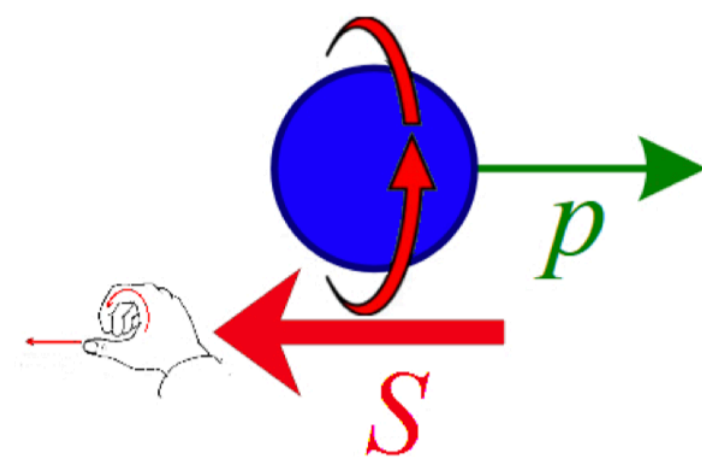
MATINS
MAGneto-Thermal evolution
of Isolated Neutron Stars

Chiral Anomaly

Right-handed



Left-handed



A particle is moving with momentum p represented by the green arrow.

— Particle Chirality —

The chirality of a particle is the projection of the spin along the direction of movement:

- right-handed if it is parallel to the movement;
- left-handed otherwise.

— Magnetic Helicity —

- Pure poloidal & toroidal components are unstable
- Both components are necessary for the stability (linked structures)
- Magnetic helicity quantify the topological stability

$$\frac{\partial (A \cdot B)}{\partial t} = -2cE \cdot B - c\nabla \cdot (E \times A)$$

— Chiral Anomaly —

- Changes in magnetic helicity create or destroy chiral asymmetry (vice versa).
- Chiral electric current induced along field lines

$$\frac{\partial n_5}{\partial t} = \frac{2\alpha}{\pi\hbar} E \cdot B - n_5 \Gamma_f$$

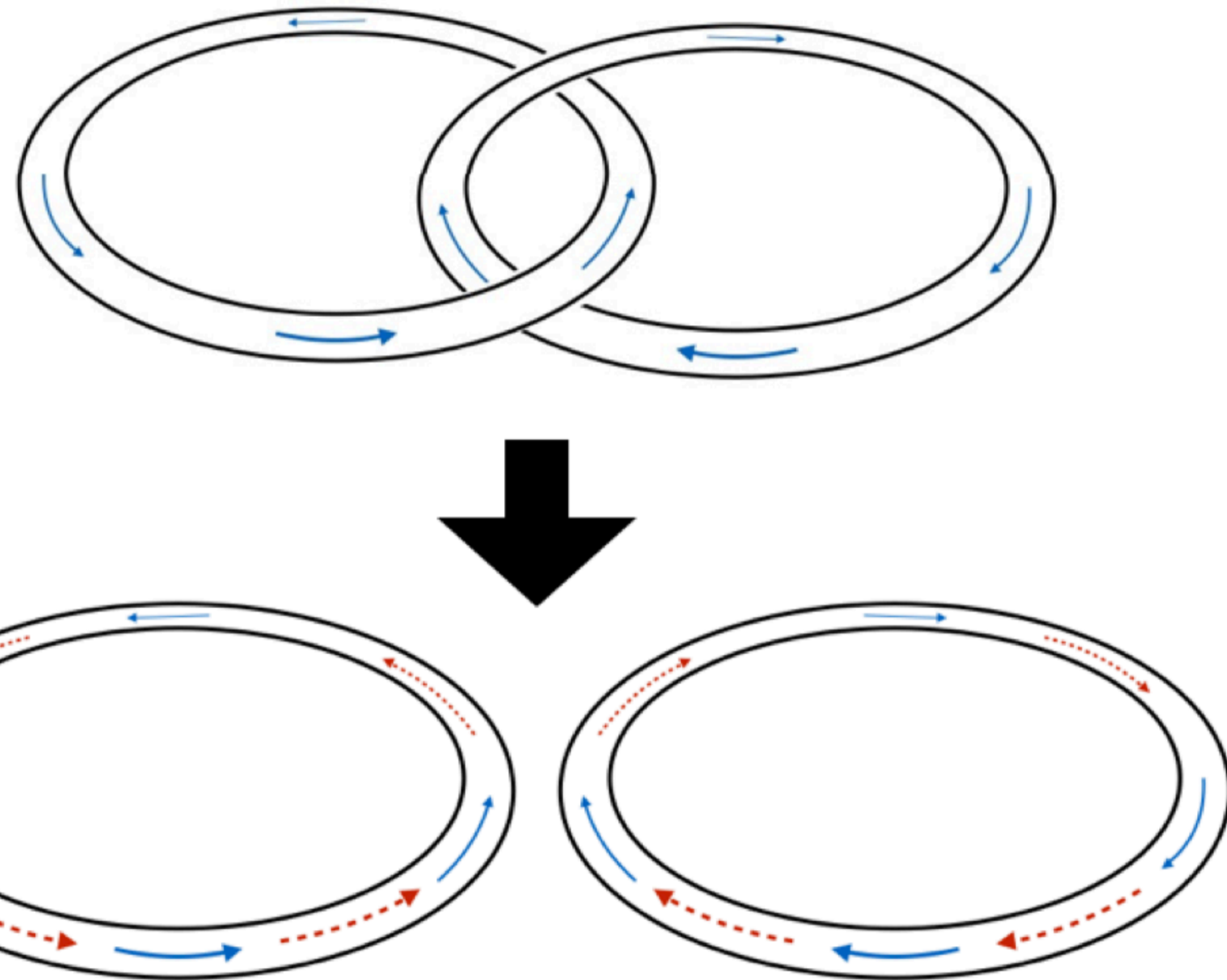
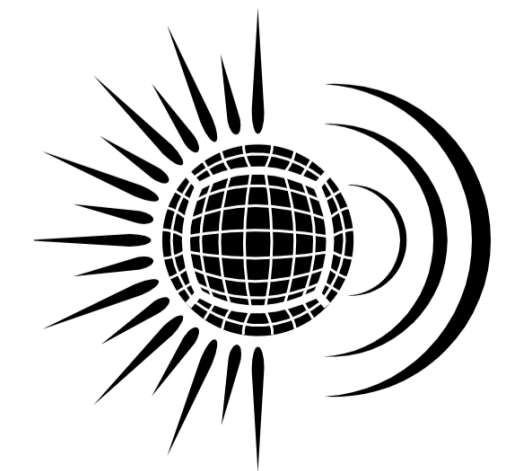
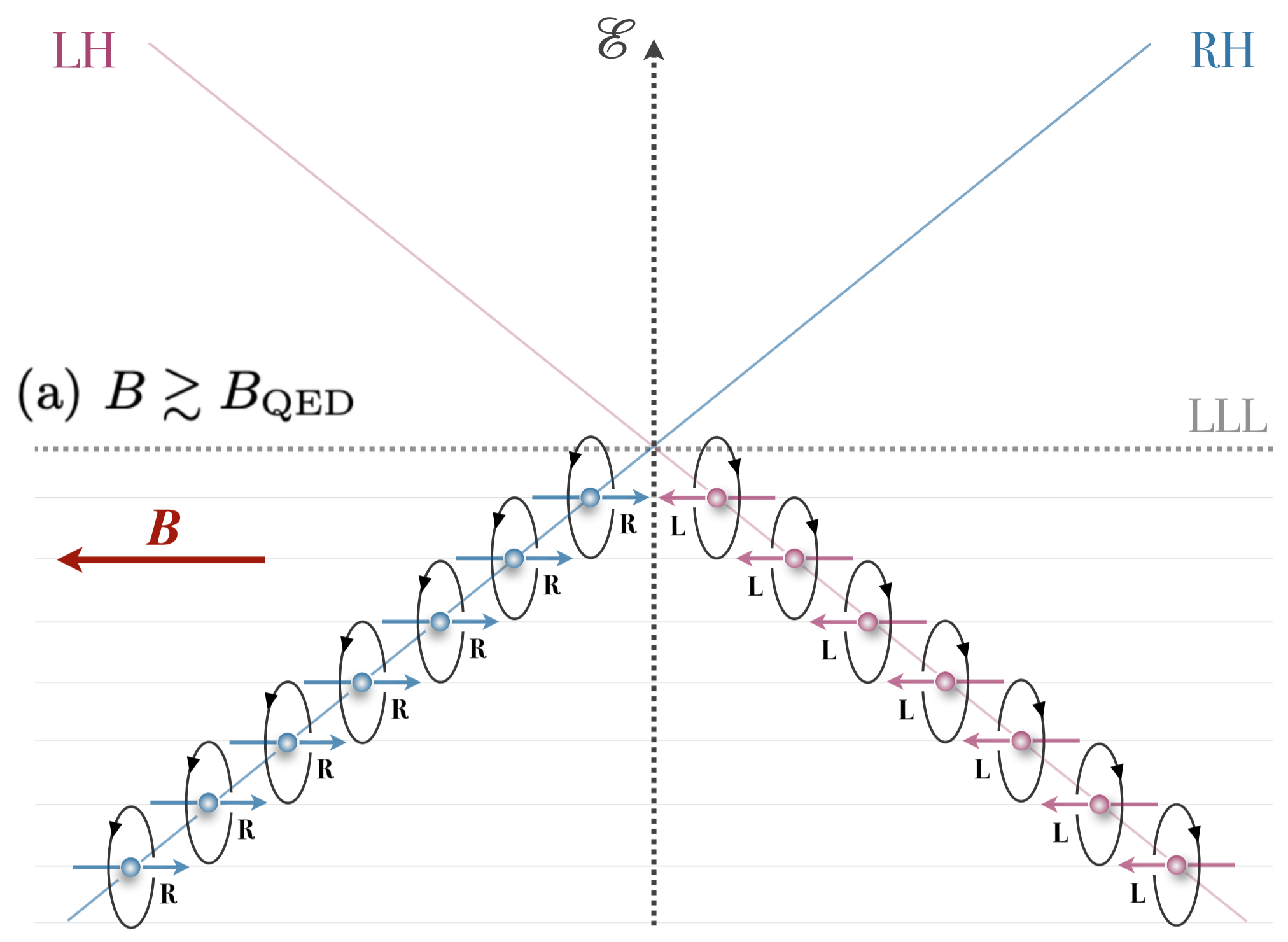
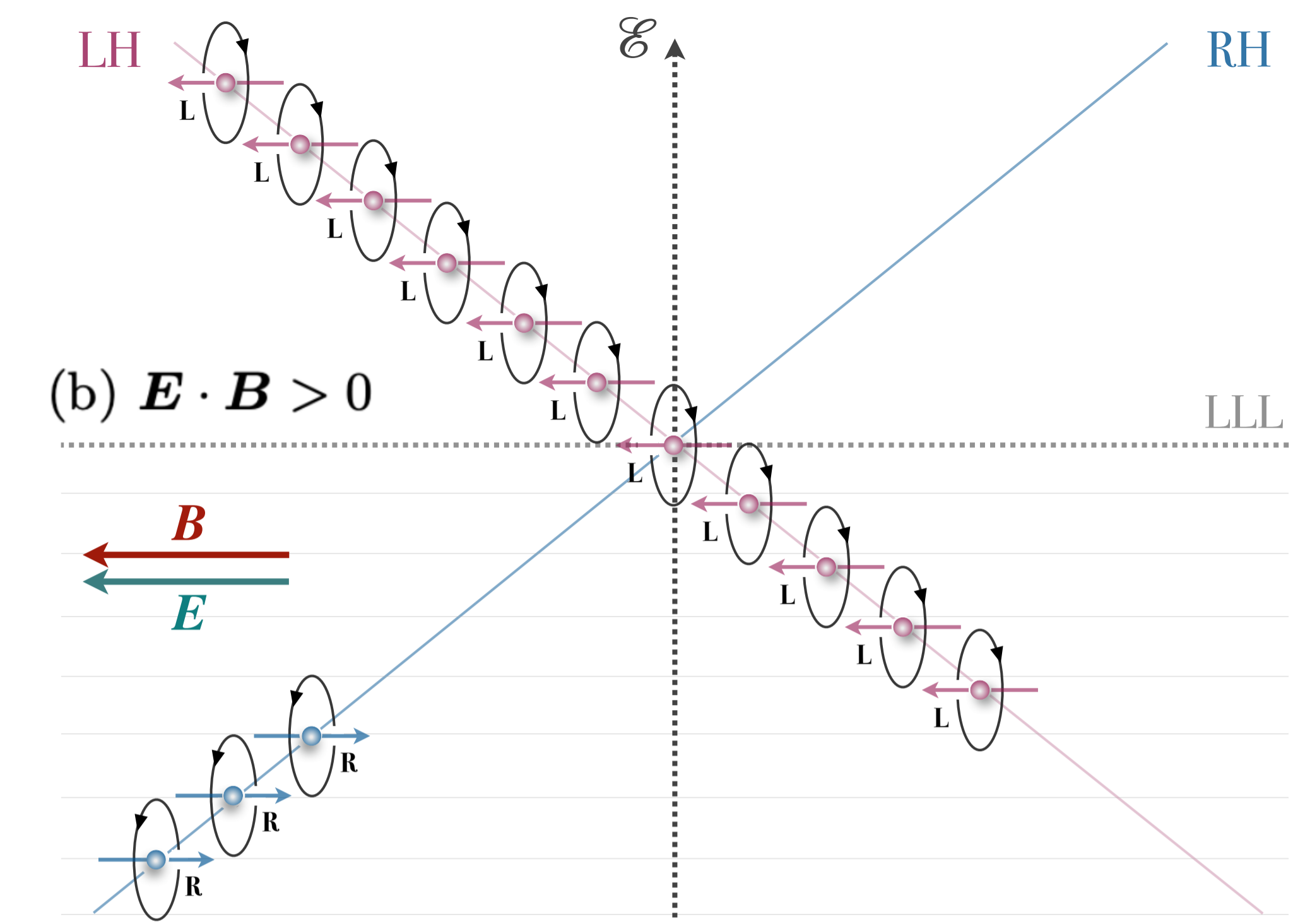
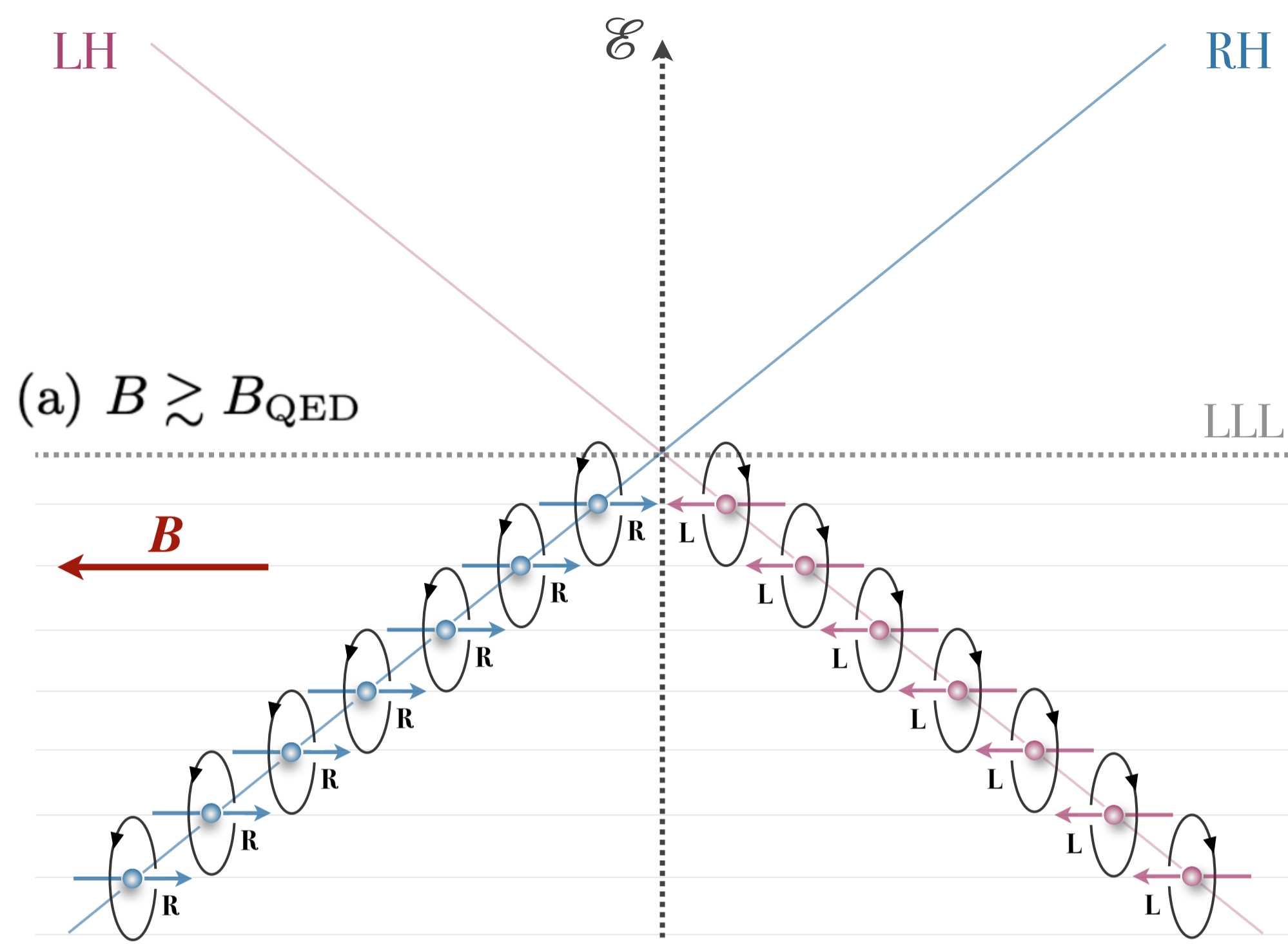
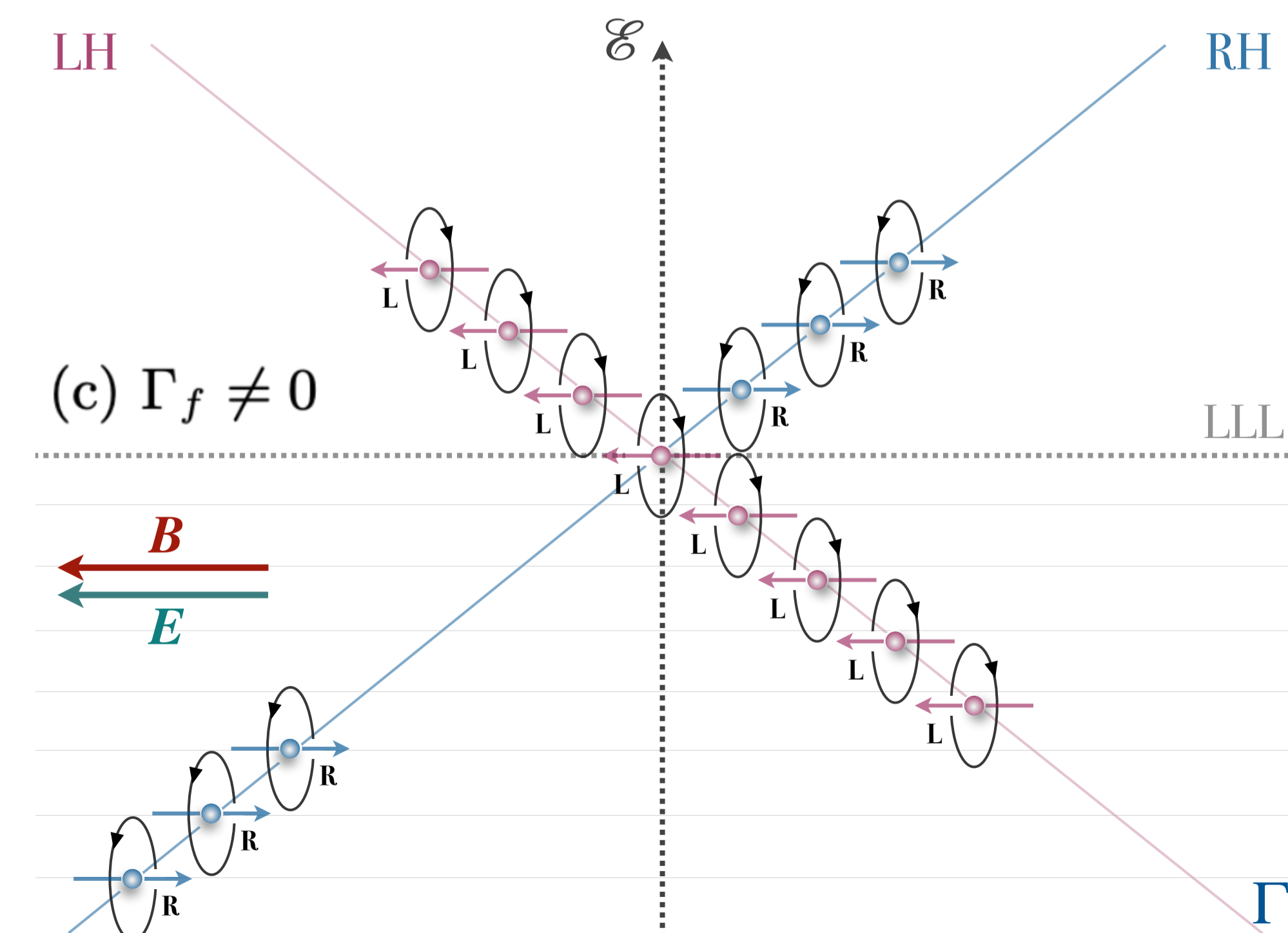
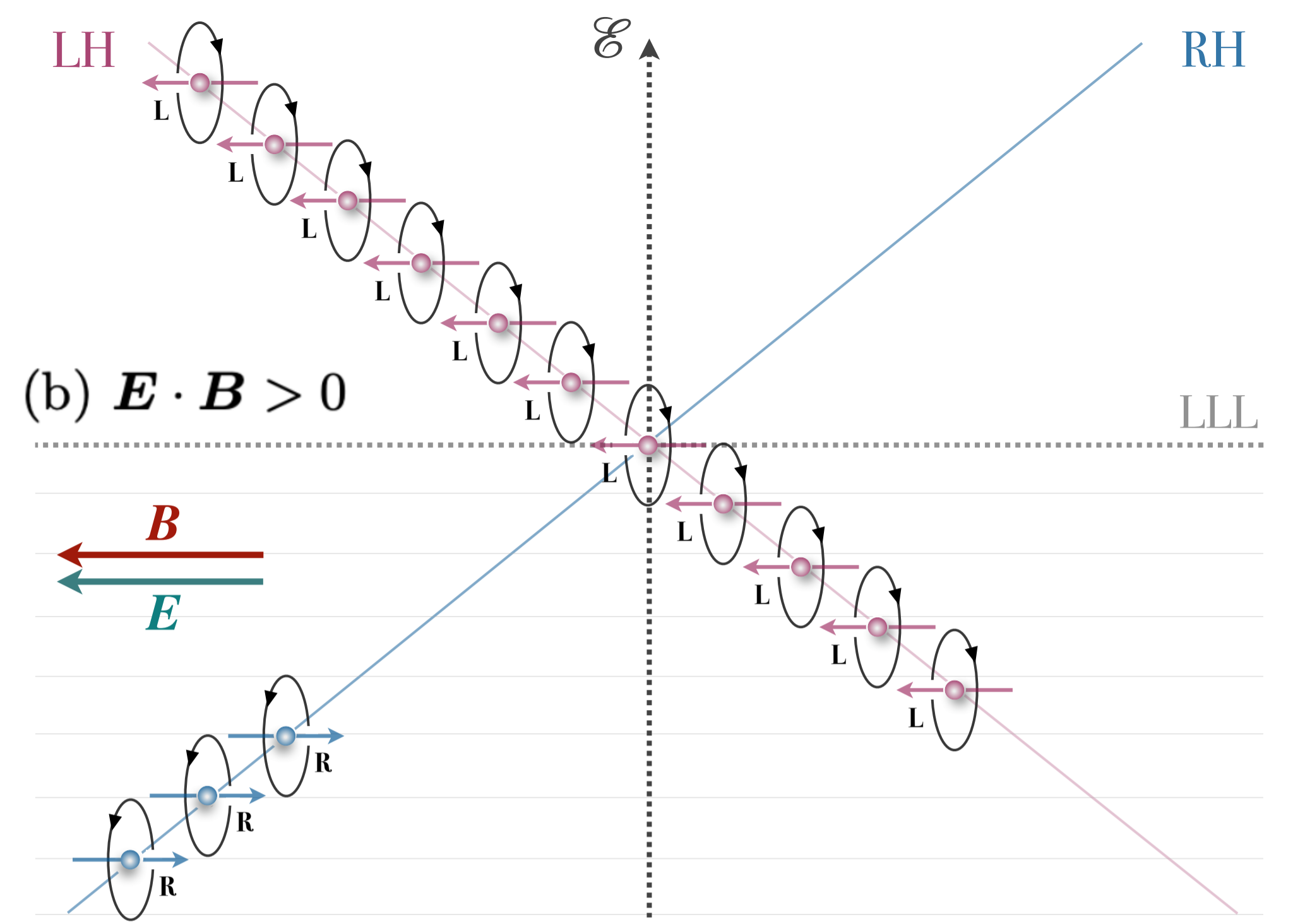
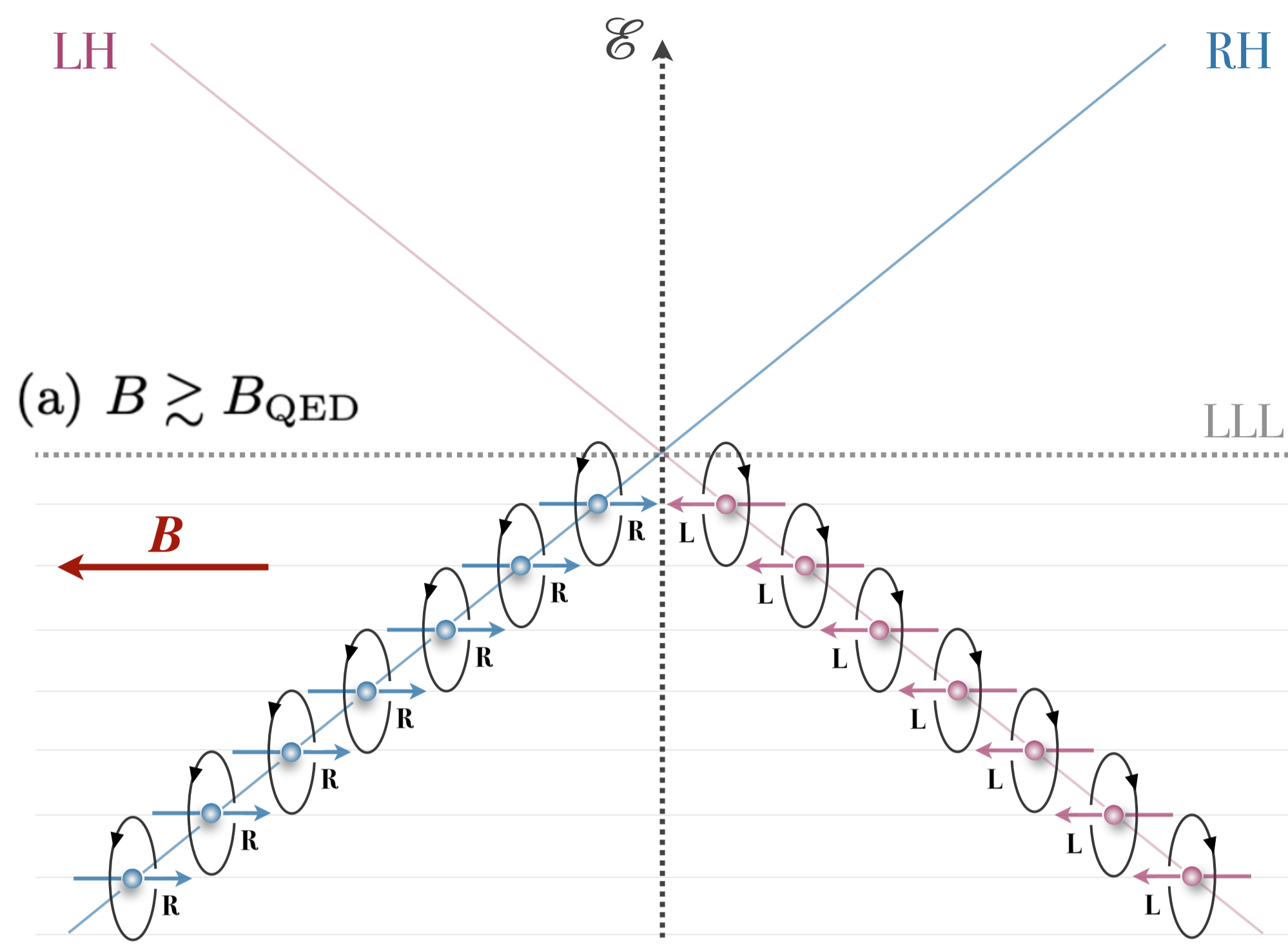


Image credit: Y. Hirono



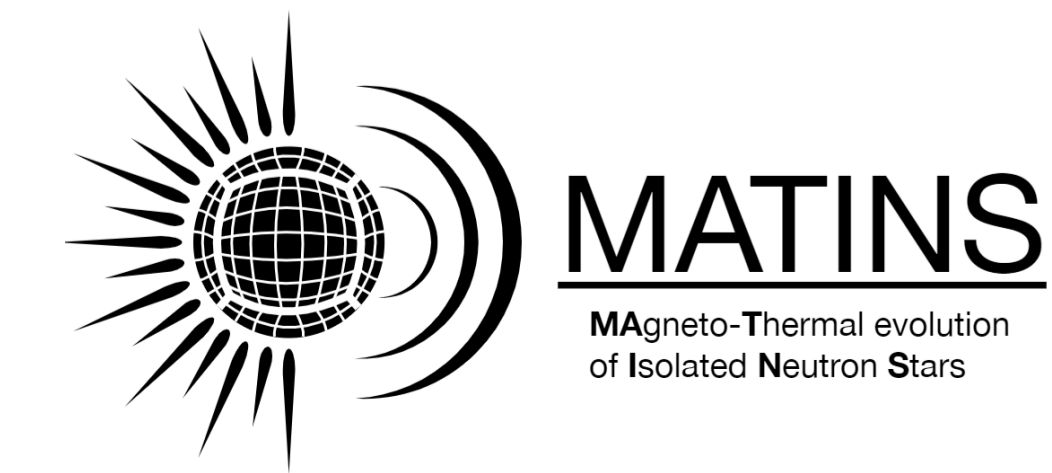


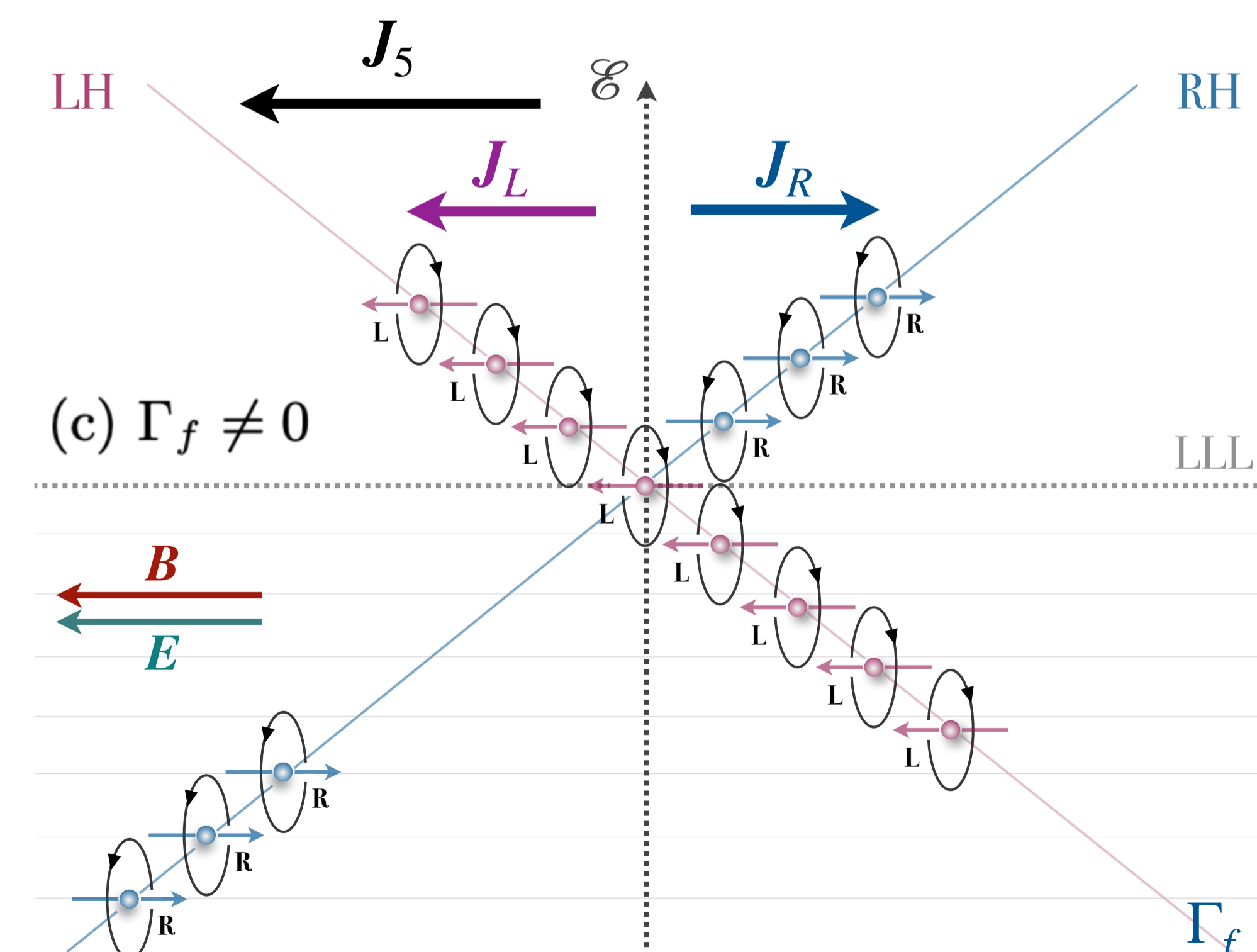
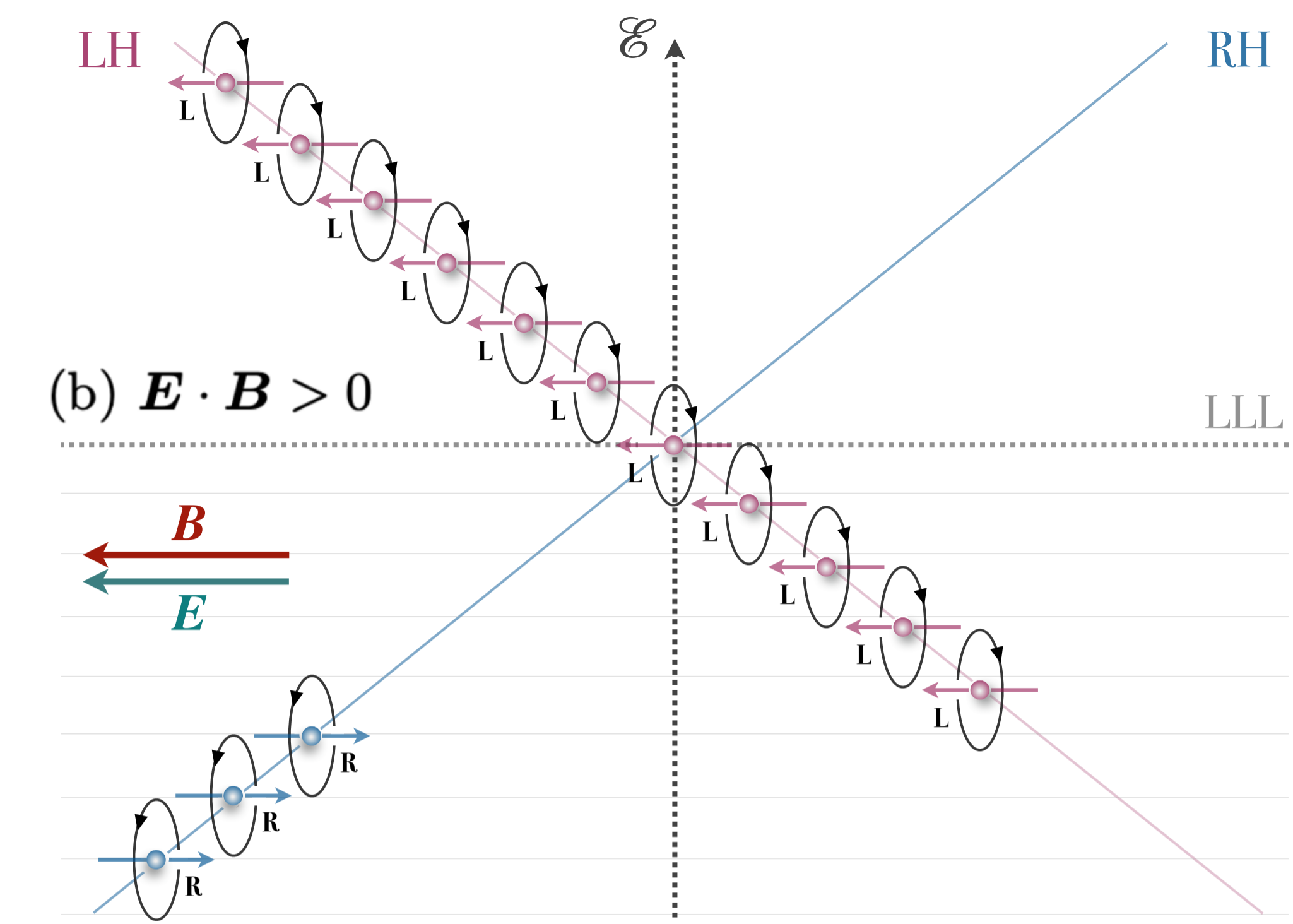
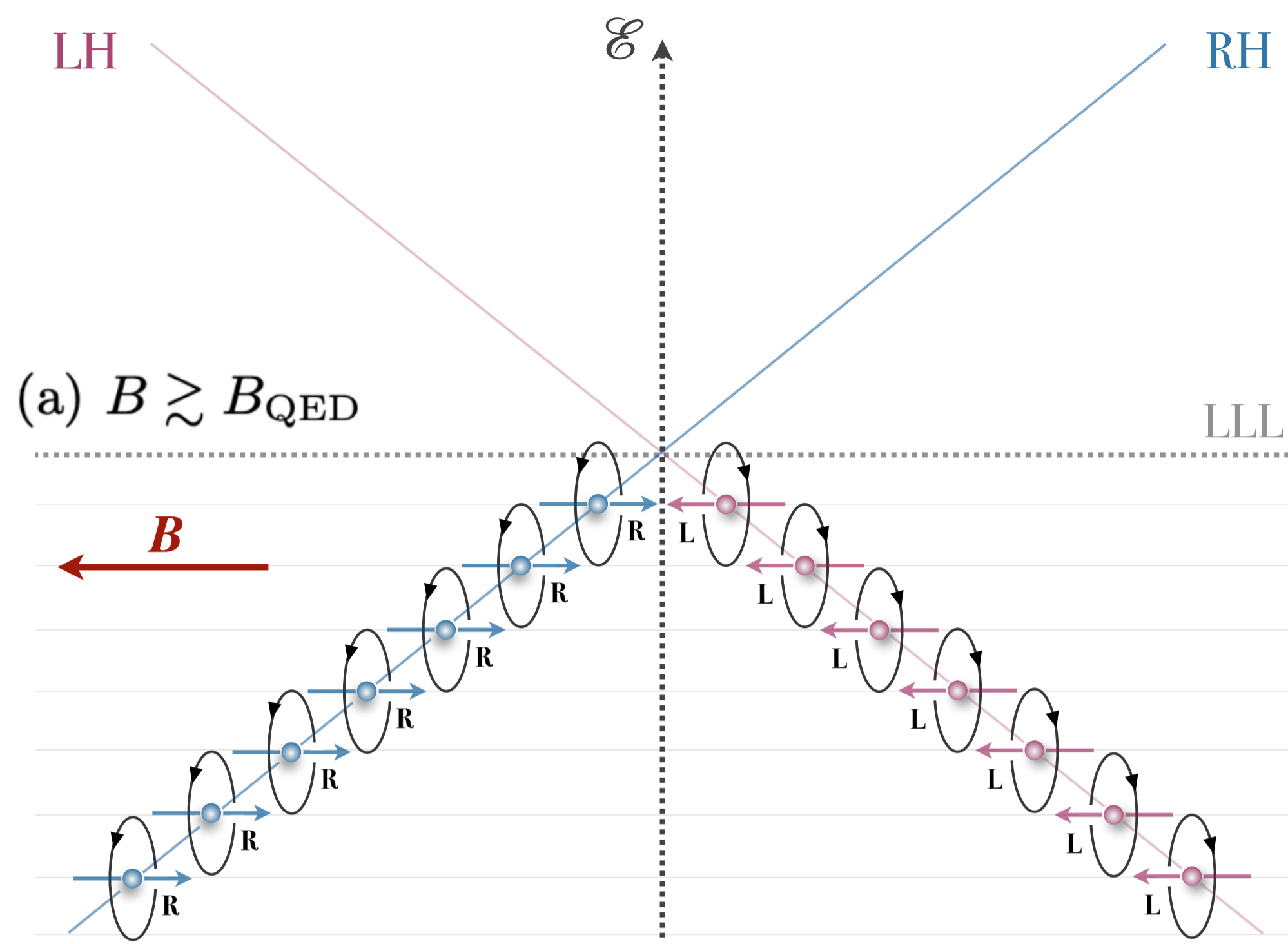




$$\Gamma_f = \left(\frac{m_e}{\mu_e} \right)^2 \nu_{\text{coll}} = \frac{4\alpha}{3\pi\sigma_e} \frac{m_e^2 c^4}{\hbar^2}$$

[Dehman 2026, arXiv: 2605.08068]





$$J_5 = J_R + J_L = \frac{\alpha}{\pi\hbar} \mathbf{B} (\mu_R - \mu_L) = \frac{\alpha\mu_5}{\pi\hbar} \mathbf{B}$$

$$|\mu_5| \approx 10^{-12} \dots 10^{-11} \text{ MeV} \ll \mu_e = 10 \dots 100 \text{ MeV}$$

$$\mathbf{J} = \frac{c}{4\pi} (\nabla \times \mathbf{B}) = \sigma_e \mathbf{E} + \mathbf{J}_5$$

$$\frac{\partial \mathbf{B}}{\partial t} = -\nabla \times [\eta \nabla \times \mathbf{B} - \eta k_5 \mathbf{B}] + f_h (\nabla \times \mathbf{B}) \times \mathbf{B}$$

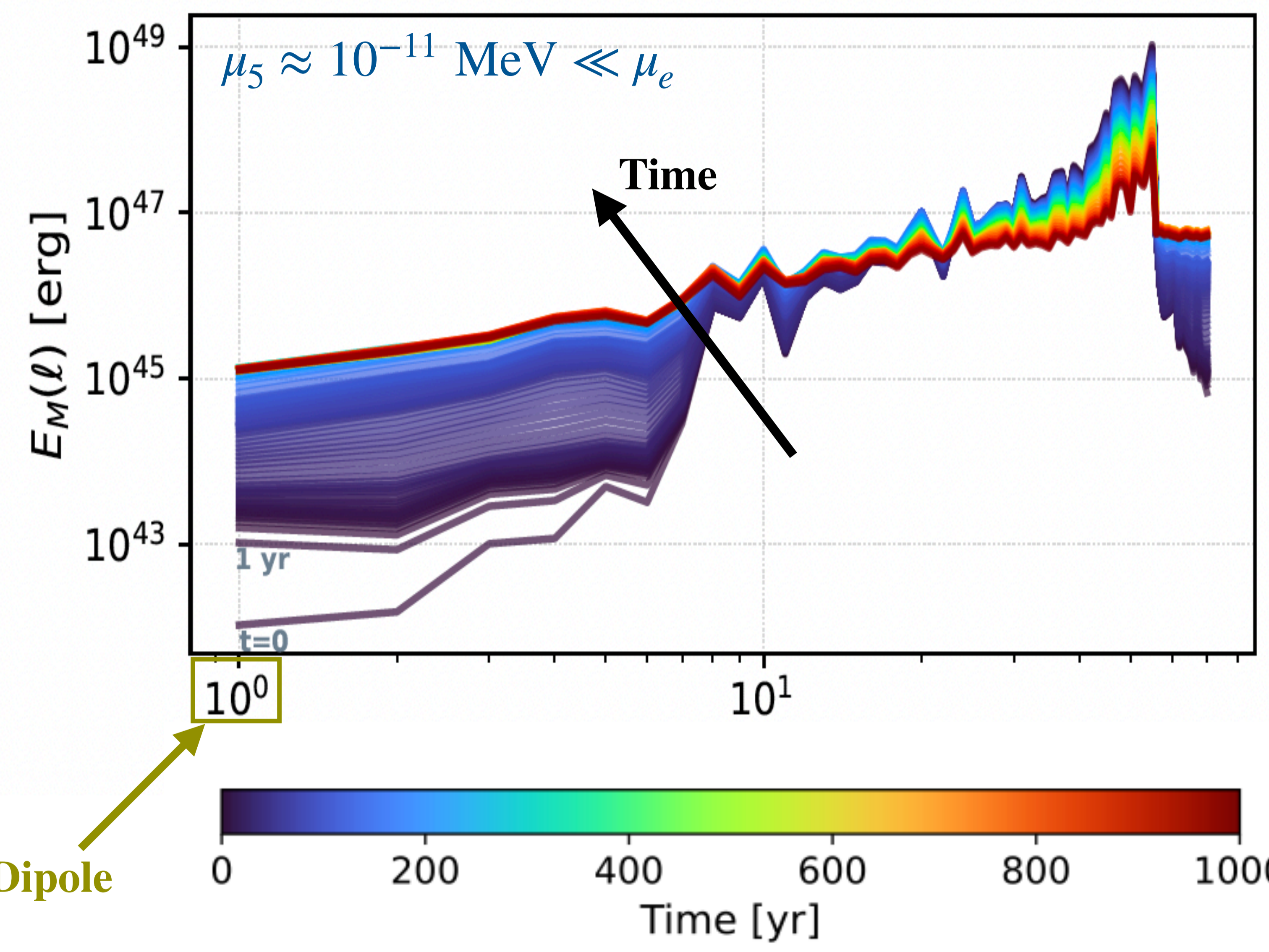
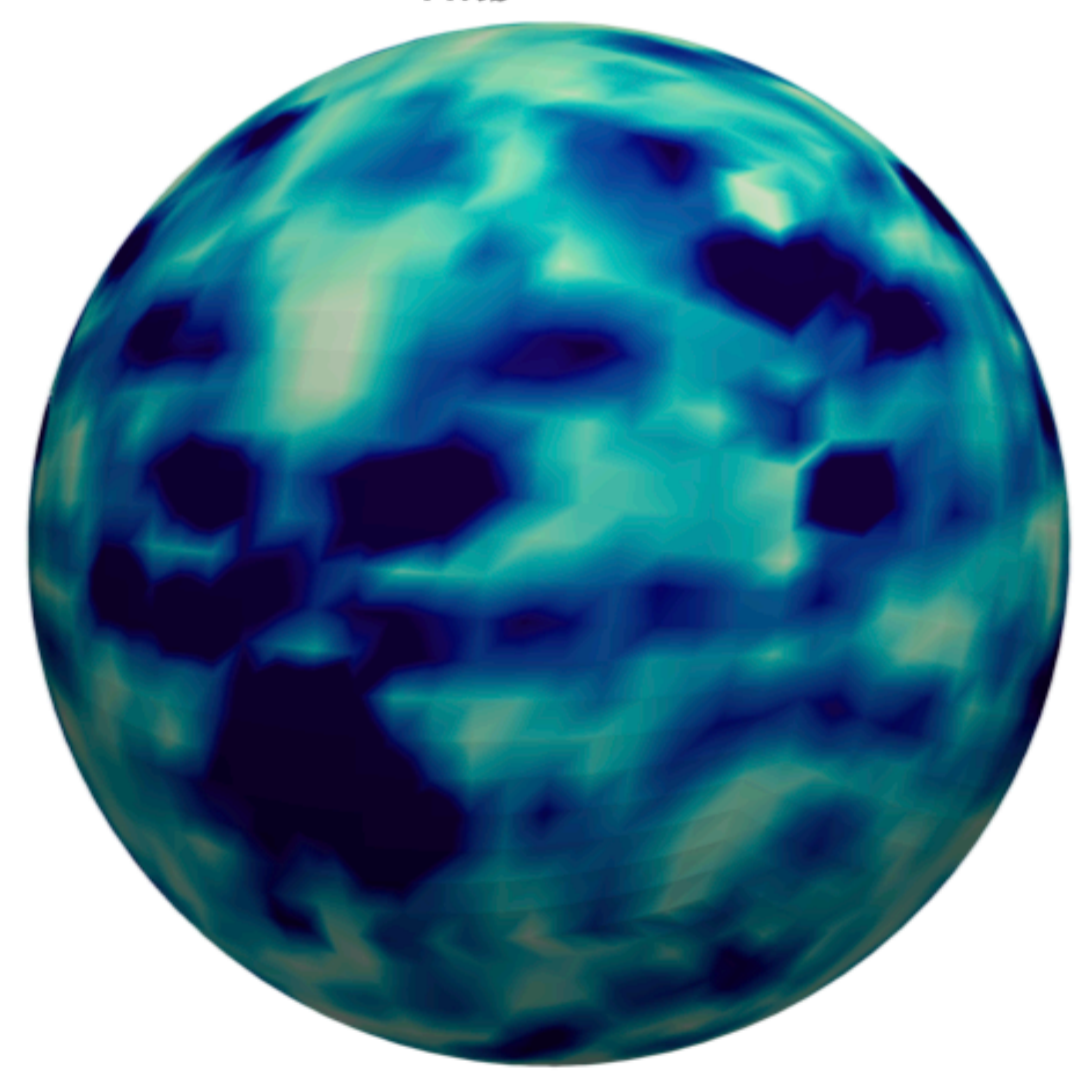
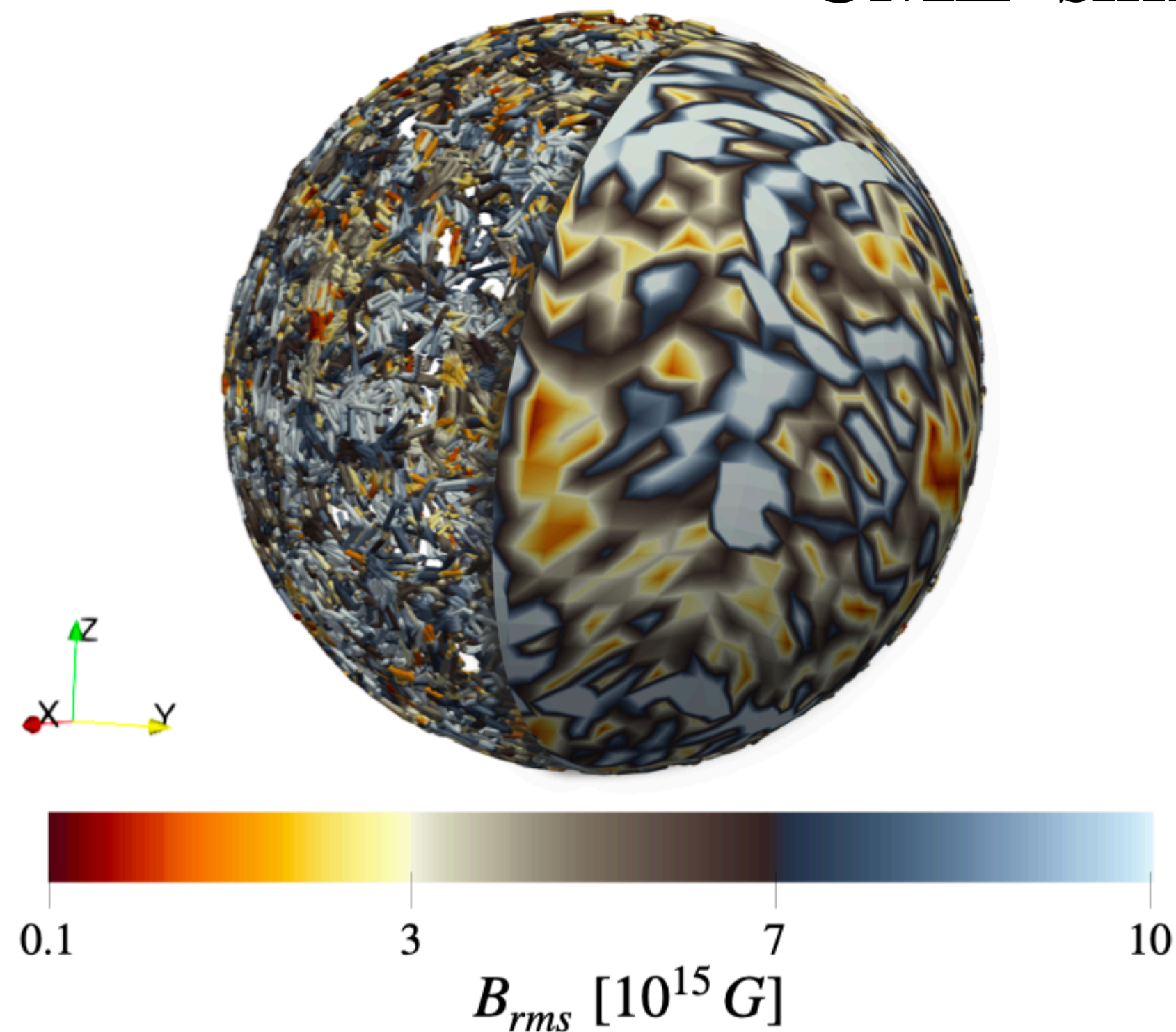
[Dehman & Pons 2025, PRR]

$$\Gamma_f = \left(\frac{m_e}{\mu_e} \right)^2 \nu_{\text{coll}} = \frac{4\alpha}{3\pi\sigma_e} \frac{m_e^2 c^4}{\hbar^2}$$

[Dehman 2026, arXiv: 2605.08068]



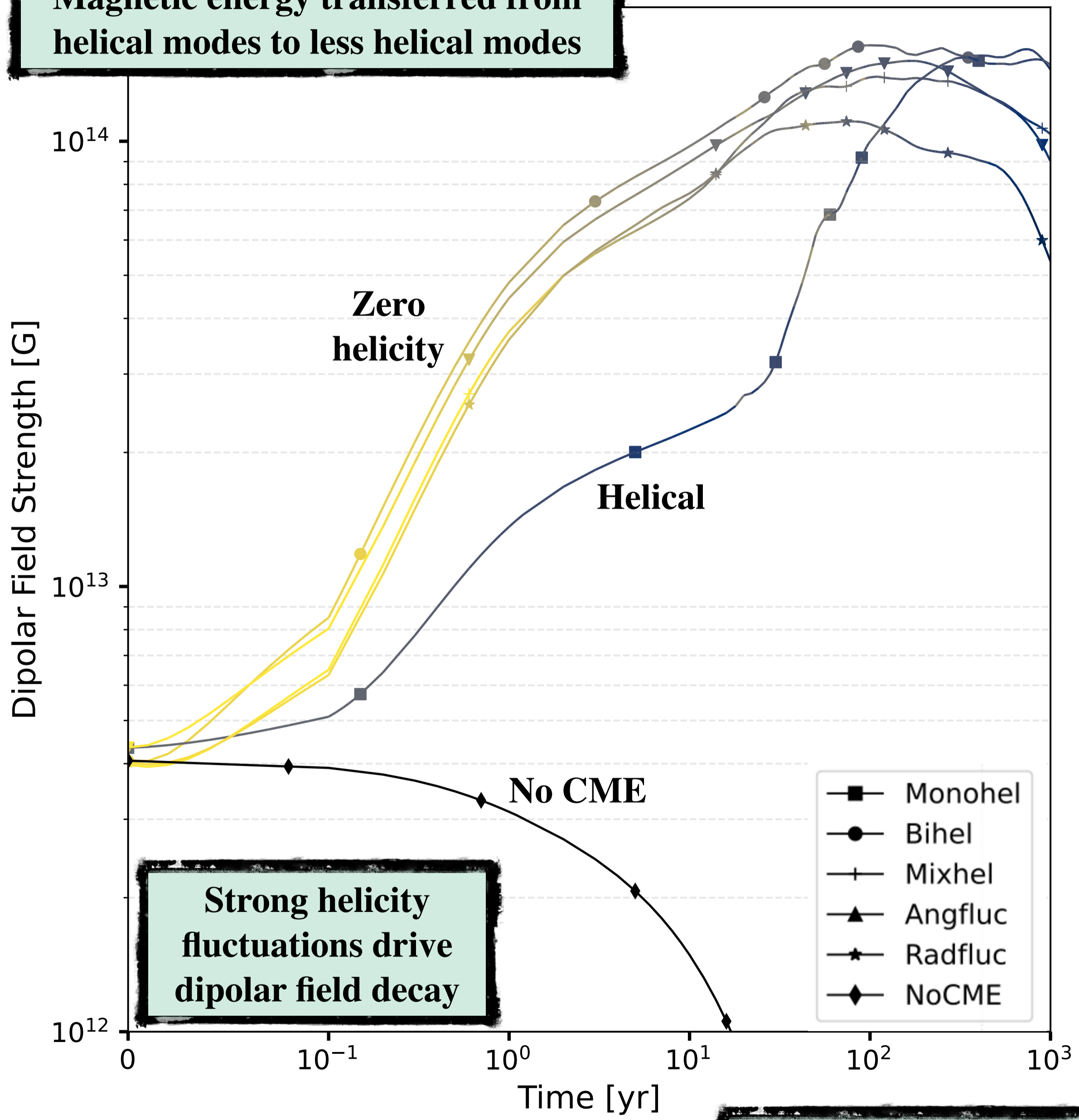
CME simulations — net magnetic helicity



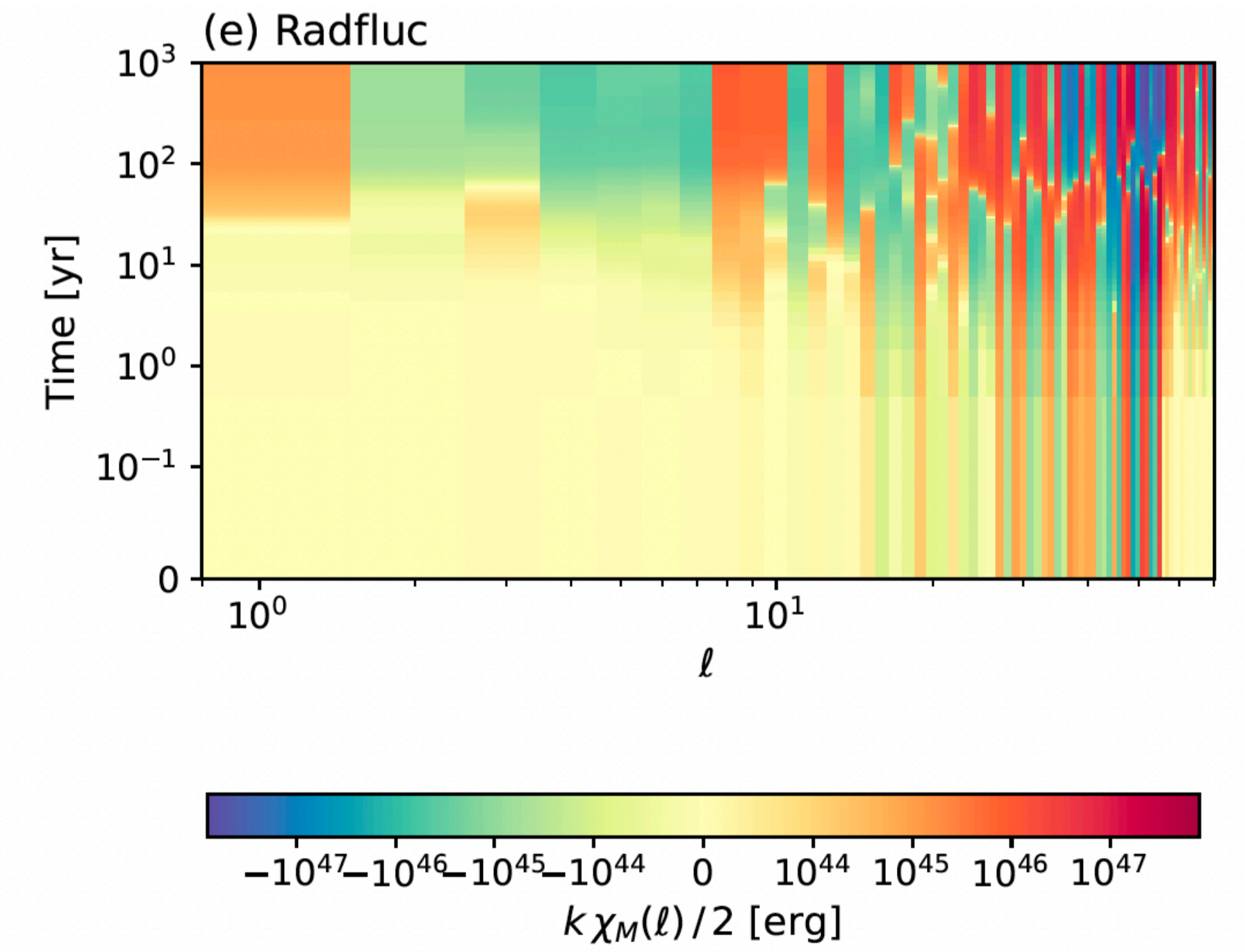
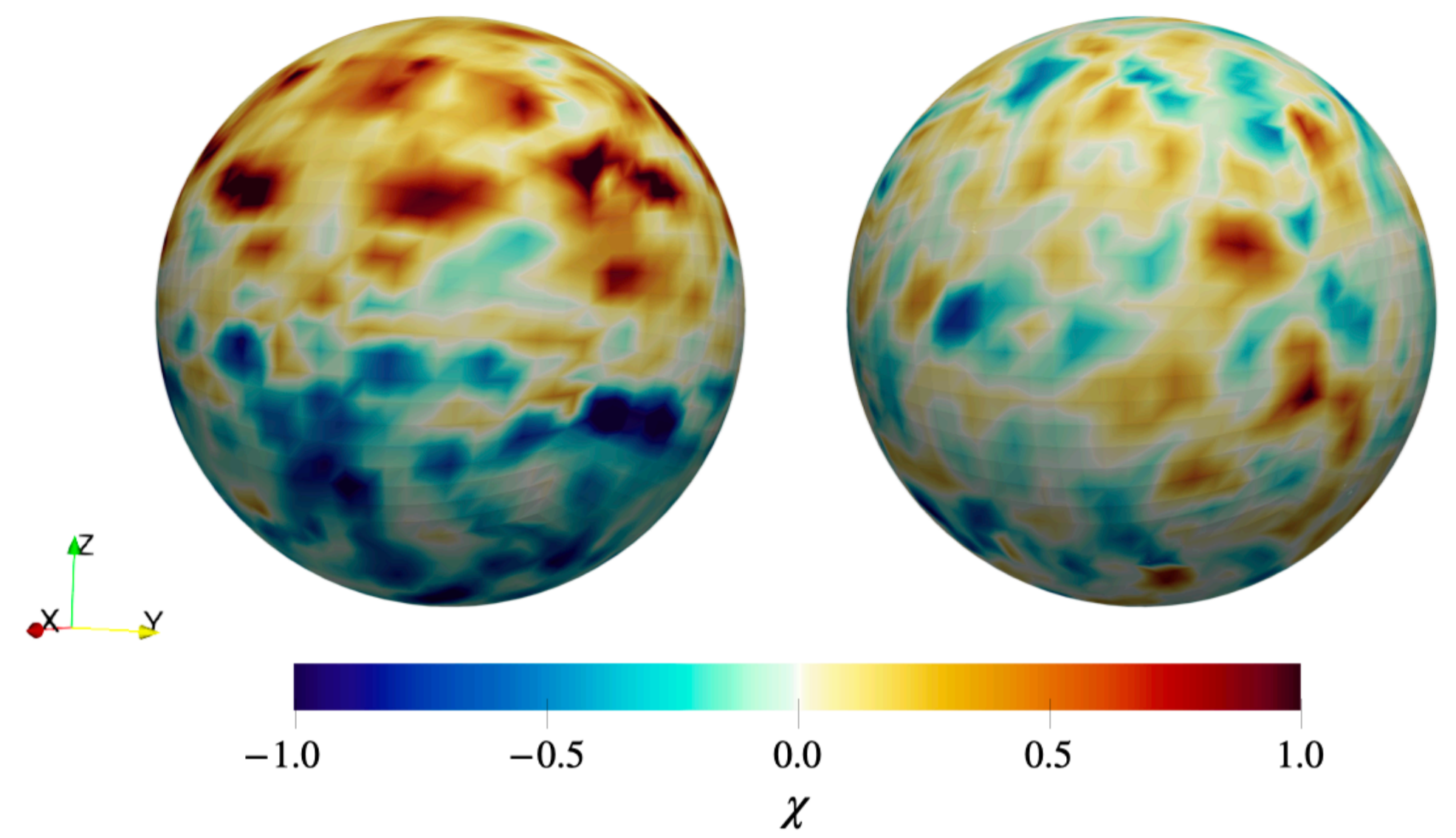
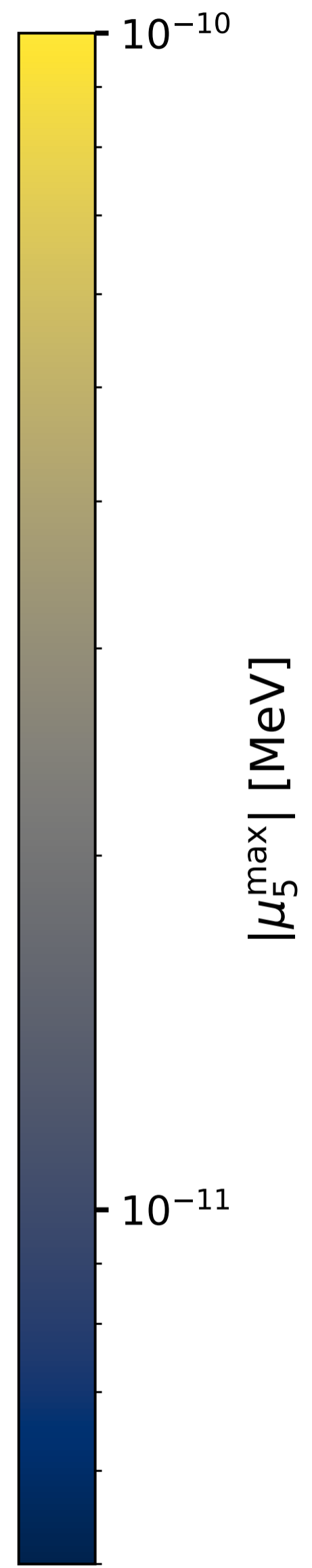
CME simulations — vanishing helicity

Onset of CMI is governed by $|\mu_5^{\max}|$

Magnetic energy transferred from helical modes to less helical modes



Strong helicity fluctuations drive dipolar field decay



CME provides a possible explanation for magnetar formation
 At birth: need **initial field (small scales)** + **helicity distribution**

[Dehman 2026, arXiv: 2605.08068]



Summary & Conclusion:

MATINS: a new 3D code for magneto-thermal evolution of isolated neutron stars, enabling self-consistent Myr-scale evolution linking magnetic fields to X-ray emission, spin-down, and magnetar activity.

Long-term evolution (10^6 yr) with a strong magnetic field $\sim 10^{14} \dots 10^{15}$ G.

Proper treatments of microphysics, envelope models, axial singularity, field structure, temperature, etc.

Hall cascade, Inverse Hall cascade, outburst, etc.

Origin of magnetic field in magnetars:

- Dynamo simulations in core-collapse simulations and proto-neutron stars.
- Inverse cascade in neutron star
- Chiral anomaly at the origin of magnetars large scale magnetic field.

NewAthena: will not measure internal magnetic fields directly, but it may provide the strongest observational constraints yet on the hidden magnetic structures that govern neutron-star evolution.

- ➔ Resolve multipolar surface magnetic fields beyond the spin-down dipole.
- ➔ Constrain hidden internal (toroidal) magnetic-field components through thermal mapping.
- ➔ Measure the impact of magnetic-field decay on neutron-star heating and evolution.

